JCI The Journal of Clinical Investigation

Tissue-resident PSGL1^{lo}CD4^{+} T cells promote B cell differentiation and chronic graft-versus-host-disease-associated autoimmunity

Xiaohui Kong, … , Aimin Huang, Defu Zeng

J Clin Invest. 2020. https://doi.org/10.1172/JCI135468.

Research In-Press Preview **Transplantation**

Graphical abstract

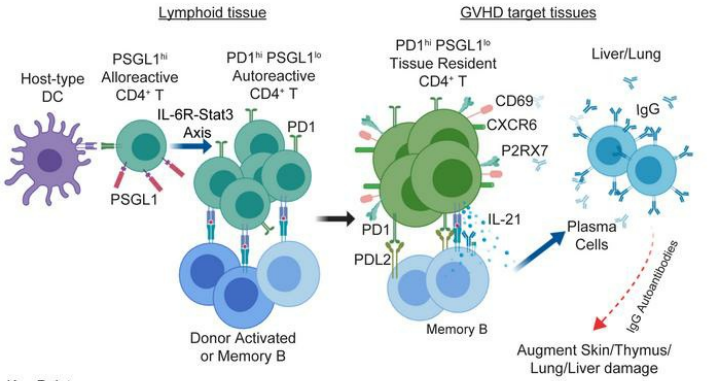

Key Point:

- Peripheral PSGL1^{hi}CD4^{+} T cells interact with host-APC in lymphoid tissue and differentiate into B cell helper of PD1^{hi}PSGL1^{lo}CD4^{+}T cells in an IL-6R-Stat3 dependent manner.
- PSGL1^{lo}CD4^{+} T cells upregulate expression of CD69, CXCR6 and P2RX7 in the GVHD target tissues and become tissue resident memory T (Trm) cells.
- PSGL1^{lo}CD4^{+} Trm interact with memory B cells via PD-1 and PD-L2, leading to the memory B cell differentiation into plasma cells that produce IgG antibodies that augment GVHD tissue damage.

Tissue-resident PSGL1^{lo}CD4^{+} T cells promote B cell differentiation and chronic graft-versus-host-disease-associated autoimmunity

Xiaohui Kong[1, 2*], Deye Zeng[1, 2,3*], Xiwei Wu[4], Bixin Wang[1,2, 5], Shijie Yang[1,2,6], Qingxiao Song[1, 2, 5], Yongping Zhu[1, 2], Martha Salas[1, 2], Hanjun Qin[4], Ubaydah Nasri[1, 2], Karen M. Haas[7], Arthur D. Riggs[1], Ryotaro Nakamura[2], Paul J. Martin[8], Aimin Huang[3$], and Defu Zeng[1, 2$]

Running Title: Tissue-resident PSGL1^{lo}CD4^{+} T cells augment chronic GVHD

1. Diabetes and Metabolism Research Institute, the Beckman Research Institute of City of Hope, Duarte 91010, CA
2. Hematologic Malignancies and Stem Cell Transplantation Institute, City of Hope National Medical Center, Duarte 91010, CA
3. Department of Pathology at School of Basic Medical Sciences, Institute of Oncology and Diagnostic Pathology Center, Fujian Medical University, Fuzhou, China4. Department of Integrative Genomics Core, The Beckman Research Institute of City of Hope, Duarte 91010, CA
4. Department of Integrative Genomics Core, The Beckman Research Institute of City of Hope, Duarte 91010, CA
5. Fujian Medical University Center of Translational Hematology, Fujian Institute of Hematology, Fujian Medical University Union Hospital, Fuzhou, China
6. Department of Hematology, Xinqiao Hospital of Army Medical University, Chongqing, China
7. Department of Microbiology and Immunology, Wake Forest School of Medicine, Winston-Salem, NC 27157
8. Fred Hutchinson Cancer Research Center, Seattle, WA 98109

∗ XH Kong and DY Zeng contributed equally.

$ Corresponding authors:

Dr. Defu Zeng
The Beckman Research Institute of City of Hope;
1500 East Duarte road
Duarte, Ca 91010
Tel: 627-218-3587; email dzeng@coh.org.

Dr. Aimin Huang
Fujian Medical University
1 Xueyuan Road, Minhou, Fuzhou, 350122, China
Tel: 86-0591-22862869; email: aimin@fjmu.edu.cn

The authors have declared that no conflict of interest exists.

Abstract:

$CD4^+$ T cells interactions with B cells play a critical role in the pathogenesis of systemic autoimmune diseases such as systemic lupus and chronic graft-versus-host disease (cGVHD). Extrafollicular $CD44^{hi}CD62L^{lo}PSGL1^{lo}CD4^+$ ($PSGL1^{lo}CD4^+$) T cells are associated with the pathogenesis of lupus and cGVHD, but their causal role has not been established. With murine and humanized $MHC^{-/-}HLA\text{-}A2^+DR4^+$ murine models of cGVHD, we show that both murine and human $PSGL1^{lo}CD4^+$ T cells from GVHD target tissues have features of B cell helpers with upregulated-expression of PD1 and ICOS and production of IL-21. They reside in non-lymphoid tissues without circulating in the blood and have features of tissue-resident memory T cells with upregulated-expression of CD69. Murine $PSGL1^{lo}CD4^+$ T cells from GVHD target tissues augmented B cell differentiation into plasma cells and production of autoantibodies via their PD1 interaction with PD-L2 on B cells. Human $PSGL1^{lo}CD4^+$ T cells were apposed with memory B cells in the liver tissues of humanized mice and cGVHD patients. Human $PSGL1^{lo}CD4^+$ T cells from humanized GVHD target tissues also augmented autologous memory B cell differentiation into plasma cells and antibody production in PD1/PD-L2-dependent manner. Further preclinical studies targeting tissue-resident T cells to treat antibody-mediated features of autoimmune diseases are warranted.

Introduction:

Systemic autoimmune diseases such as SLE and chronic GVHD (cGVHD) are mediated by abnormal $CD4^+$ T cell interaction with B cells and autoantibody deposition in target tissues such as kidney and skin (1-4). The exacerbated autoimmunity in SLE is associated with enlarged germinal centers (GC) in which T follicular helper (Tfh) cells interactions with GC B cells lead to the production of long-lived plasma cells and high-affinity IgG antibodies with somatic hyper-mutation (5). Tfh cells express high levels of PD1 that interact with PD-L2 on GC B cells to augment antibody production (6), although $PD1^{-/-}$ mice still develop autoimmune syndromes with high concentrations of autoantibodies in the serum (7).

P-selectin glycoprotein ligand 1 (PSGL1, also known as CD162) is widely expressed in almost all T cells in the blood and binds to E-selectin and P-selectin after appropriate glycosylation and tyrosine sulfation, which regulates migration of immune cells into tissues (8). A subset of activated $CD4^+$ T cells in the spleen of SLE mice downregulate expression of PSGL1, and they become $CD44^{hi}CD62L^-PSGL1^{lo}CD4^+$ T ($PSGL1^{lo}CD4^+$ T) cells (9). $PSGL1^{lo}CD4^+$ T cells localize at the extrafollicular sites of systemic lupus mice, they express high levels of CXCR4, ICOS and CD40L without expression of CXCR5 (1). Unlike germinal center $CXCR5^+$Tfh $CD4^+$ T cell development, $CXCR4^+PSGL1^{lo}CD4^+$ T cells develop outside germinal centers in an ICOS-dependent manner (9). $PSGL1^{lo}CD4^+$ T cells from the spleen of SLE mice augment auto-antibody production through IL-21 and CD40L in vitro, and they have been designated as extra-follicular B cell helpers (Tefh) (1, 9). However, whether $PSGL1^{lo}CD4^+$ T cells interact with B cells in non-lymphoid tissues of autoimmune mice remains unclear. In addition, $PSGL1^{lo}CD4^+$ T cells in humans have yet not been reported.

cGVHD often occurs as a sequela of acute GVHD (aGVHD)(10). GVHD is a severe side effect of allogeneic hematopoietic cell transplantation (allo-HCT) in which alloreactive T cells attack target organs such as gut, liver, lung and skin (11). Acute GVHD is an acute inflammatory response mainly mediated by infiltrating alloreactive T cells, while cGVHD is mediated by auto-reactive $CD4^+$ T cells derived from T cells in the graft (12-14) and from failure of negative selection in the thymus (15, 16), by aberrant B cell signaling (17) and by abnormal $CD4^+$ T and B interactions due to lack of donor-derived Treg cells (2, 18). $CD4^+$ T cell interaction with B cells augments cGVHD via clonal expansion of pathogenic $CD4^+$ T cells and autoantibody production (4).

Others have reported that cGVHD pathogenesis was associated with enlarged germinal centers (GCs) and that BCL6 deficiency in donor B cells prevented cGVHD (19). We recently reported that cGVHD causes destruction of lymphoid follicles and absence of GCs in the lymphoid tissues (20). cGVHD pathogenesis did not require donor B cell expression of BCL6 or GC formation, and development of the disease was associated with the expansion of extrafollicular $CXCR5^-BCL6^+PSGL1^{lo}CD4^+$ T cells in GVHD target tissues (20). Our previous study left several important questions unanswered. How do $PSGL1^{lo}CD4^+$ T cells in the GVHD target tissues interact with B cells? Do $PSGL1^{lo}CD4^+$ T cells circulate in the blood? To what extent do murine and human $PSGL1^{lo}CD4^+$ T cells from GVHD target tissues have a similar phenotype and function?

Tissue-resident memory T (Trm) cells are $CD44^{hi}CD62L^-$ with high expression of CD69, CD103, CD49a, CD101and P2RX7, but low expression of KLF2/3, S1PR1, and CCR7 (21). The low expression of S1PR1, CCR7 and CD62L restricts their egress from tissues into the circulation and ensures their residency in tissues (21). In addition, Blimp1 and Hobit, Runx3 and Notch are transcription factors that regulate Trm development and maintenance(21). Trm cells in healthy

tissues serve as a front line of defense against pathogens in the gut, skin and lung (22). Trm cells also play an essential role in inducing local humoral responses by recruiting B cells during infection (23). Previous studies have not established whether Trm cells interact directly with B cells.

Autoimmune-like cGVHD can emerges after aGVHD or emerges after HCT without preceding aGVHD (16, 18, 24). In the current studies, we used a murine model of cGVHD that emerges after aGVHD (16) and a newly established humanized $MHC^{-/-}HLA\text{-}A2^{+}DR4^{+}$ mouse model of cGVHD to show that tissue-resident murine and human $PSGL1^{lo}CD4^{+}$ T cells augment memory B cell differentiation into plasma cells and production of autoantibody in a PD1- and PD-L2-dependent manner.

Results

Expansion of PSGL^{lo}CD4^{+} T cells is observed in the liver and lungs of recipients with overt cGVHD but not in those with mild cGVHD.

We induced overt cGVHD and mild cGVHD by injecting spleen cells (1.0 or 0.1 x10^6) and T cell-depleted bone marrow cells (TCD-BM, 2.5x10^6) from MHC-mismatched C57BL/6 donors into lethal TBI-conditioned BALB/c recipients, as previously described (16, 20). Recipients given TCD-BM alone were used as GVHD-free controls. Recipients given 1x10^6 spleen cells developed overt cGVHD with bodyweight loss, hair-loss and mortality, and ~37% survived for more than 60 days. Recipients given 0.1x10^6 donor spleen cells developed mild cGVHD with some weight-loss, but no clear hair-loss or mortality, and all survived for more than 60 days (Supplemental Figure 1A). Although the numbers of PSGL1^{lo}CD4^{+} T cells were not increased in the liver, they were significantly increased in the lung at 60 days after HCT in recipients with mild cGVHD when compared to GVHD-free recipients, but they were greatly expanded in both liver and lung of recipients with overt cGVHD (Supplemental Figure 1B). As indicated by the presence of Tfh cells and GC B cells, splenic germinal centers (GCs) persisted in recipients with mild cGVHD but could not be detected in recipients with overt cGVHD (Supplemental Figure 1C).

PSGL1^{lo}CD4^{+} T cells are absent in the peripheral blood and skin but expanded in the liver and lungs of overt cGVHD recipients.

At 60 days after HCT, recipients with overt cGVHD had moderate cellular infiltration and clear collagen deposition in the liver, lung, skin, and salivary gland, as well as IgG antibody deposition in the liver, lung, skin and thymus tissues (Supplemental Figure 2, A-C). The percentage and yield of PSGL1^{lo}CD4^{+} T cells were much higher in the liver and lungs of cGVHD recipients as compared with GVHD-free recipients. PBMC and skin-MNC from GVHD-free or cGVHD recipients contained few PSGL1^{lo}CD4^{+} T cells, with no differences between the two groups. The

percentage and yield of PSGL1^{lo}CD4^{+} T cells among MNC from intestinal tissues were low in GVHD-free and cGVHD-recipients, with no difference between the two groups (Figure 1, A and B). At the onset of cGVHD, 30 days after HCT, PSGL^{lo}CD4^{+} T cells were not detectable in the blood or skin, either, while the percentage and yield of PSGL1^{lo}CD4^{+} T cells were much higher in the liver and lung of cGVHD recipients as compared with GVHD-free recipients (Supplemental Figure 3, A and B). While donor-derived B cells were present in the liver of GVHD-free and cGVHD recipients on days 30 and 60 after HCT, they were nearly absent in the skin (Supplemental Figure 3C).

PSGL^{lo}CD4^{+} T cells in the GVHD target tissues are tissue-resident memory T cells.

At day 30 after HCT, nearly all PSGL1^{lo}CD4^{+} T cells in the liver and lungs were derived from the donor CD4^{+} T cells in the graft. By day 60, PSGL1^{lo}CD4^{+} cells derived from the marrow still accounted for small percent (Supplemental Figure 4, A and B). The absence of PSGL1^{lo}CD4^{+} T cells in the blood circulation and their CD62L^{-}CD44^{hi} T effector memory phenotype (Tem) suggested that they could be tissue-resident memory T (Trm) cells. Trm cells are characterized by high expression of CD69, CD103, CXCR6 and P2RX7, but low expression of CCR7 and S1PR1 (21).

To test the hypothesis that PSGL1^{lo}CD4^{+} T cells in cGVHD target tissues represent Trm cells, we compared the RNA-seq profile of sorted splenic PSGL1^{lo}CD4^{+} T cells from GVHD-free and cGVHD recipients at 30 days after HCT. PSGL1^{lo}CD4^{+} T cells from cGVHD recipients expressed typical Trm markers, with high expression of mRNA for *Cd69, Cxcr6, P2rx7* and *Il7ra* and low expression of mRNA for *Ccr7, S1pr1, Klrg1*, and *Klf2*, although we found little difference in expression of *Cd49a*, as compared with PSGL1^{lo}CD4^{+} T cells from GVHD-free recipients (Fig 1C). Flow cytometry validated that PSGL1^{lo}CD4^{+} T cells from cGVHD recipients had high expression of CD69, CXCR6 and P2RX7 and low expression of CCR7, with little difference in

CD49a expression (Figure 1D, Supplemental Figure 5). These results indicate that PSGL1^{lo} CD4^{+} T cells in cGVHD target tissues are Trm cells derived predominantly from mature T cells in the graft.

PSGL1^{lo}CD4^{+} T cells are PD1^{hi}CXCR5^{-} B cell helpers

Our previous studies suggested that extrafollicular PSGL1^{lo}CD4^{+} T cells in GVHD target tissues might have B cell helper function, because the absence of PSGL1^{lo}CD4^{+} T cells in the recipients was associated with reduction of anti-dsDNA autoantibodies (20). Consistently, in the current studies, with immunohistochemistry staining and immunofluorescent staining, we observed apposed CD4^{+} T cells and B cells in the liver and lung tissues of cGVHD recipients but only scattered CD4^{+} T and B cells in the tissues of GVHD-free recipients (Figure 2, A-D). We also observed PSGLl$^{lo/-}$CD4^{+} T cells apposed with PSGL1$^{hi/+}$B cells (Figure 2E). Many B cells juxtaposed to the CD4^{+} T cells appeared to be PD-L2^{+} memory B cells (Figure 2F). These results suggest that PSGL1^{lo}CD4^{+} T cells interact with B220^{+} B cells and also PD-L2^{+} memory B cells in the target tissues of cGVHD mice.

We compared gene expression and cell surface receptor profiles of PSGL1^{lo} and PSGL1^{hi}CD4^{+} T cells from cGVHD mice. PSGL1^{lo}CD4^{+} T cells and PSGL1^{hi}CD4^{+} T cells in the spleen, liver and lung had numerous differentially expressed genes (Figure 3, A and B). In at least 2 of the 3 organs, PSGL1^{lo}CD4^{+} T cells had high expression levels of genes for surface receptors related to T-B interactions, including *Pd1, Icos, Cd40l, Slamf6* and *Cxcr5*, and low expression levels of genes for surface markers related to anergy/exhaustion, including *Tim3* and *Lag3* (Figure 3C). They also had high expression levels of genes for nuclear factors *Maf, Stat3* and *Bcl6*, but low expression levels of genes for *Eomes* and *Tbet*. They had high expression levels of genes for *Il2, Cxcl13* and *Il21* but low expression levels of genes for *Ifng* (Figure 3C). Differential expression levels of protein for surface receptors (i.e. PD1, ICOS, CD40L, and SLAMF6),

nuclear factors (i.e., MAF), and cytokines (i.e. IL21, IFNγ and IL13) was validated by flow cytometry (Figure 3, D-F; and Supplemental Figure 6, A-D).

Although the general gene expression profiles of PSGL1^{lo}CD4^{+} T cells from the spleen, liver and lung appear to be similar (Figure 3C), a more in-depth analysis showed that the PSGL1^{lo}CD4^{+} T cells from GVHD target tissues liver and lung had high activation of KEGG pathways such as cytokine-cytokine receptor interaction pathway and graft-versus-host disease pathway, as compared to PSGL1^{lo}CD4^{+} T cells from the spleen (Supplemental Figure 6, E-G). In cGVHD recipients, PSGL1^{lo}CD4^{+} T cells from the liver had higher expression of chemokine receptors such as Ccr5, Cxcr3 and Cxcr6 than those from the spleen (Supplemental Figure 6G), consistent with our previous report that donor T cell migration into different tissues is guided by their expression of chemokine receptors and corresponding chemokines from the target tissues (25).

Since Tfh cells from the spleen of GVHD-free recipients were also mostly PSGL1^{lo} (Supplemental Figure 7), we compared PSGL1^{lo}CD4^{+} T cells with the Tfh cells as well as with PSGL1^{hi} and naïve CD4^{+} T cells. We found that PSGL1^{lo}CD4^{+} T cells expressed lower levels of PD1, ICOS, SLAMF6 and MAF than that of Tfh cells; in contrast, as compared with PSGL1^{hi} CD4^{+} T cells, PSGL1^{lo}CD4^{+} T cells expressed significantly higher levels (Figure 3, D and E; and Supplemental Figure 6, A and B). Although PSGL1^{lo}CD4^{+} T cells from cGVHD recipients had higher expression levels for both *Pd1* and *Cxcr5* mRNA as compared with PSGL1^{hi}CD4^{+} T cells, they had only higher expression levels of PD1, with little expression of CXCR5, as measured by flow cytometry (Figure 3, C and D; and Supplemental Figure 6A). Although PSGL1^{lo}CD4^{+} T cells have higher expression levels of PD1, they had lower expression levels of other anergy/ exhaustion markers such as LAG3 and TIM3 and lower expression levels of the terminal differentiation marker KLRG1 and the T cell marker IL7R (Figure 3G). Therefore, Consistent

with report that PD1 expression level alone is not associated with alloreactive T cell anergy/ exhaustion status (26), these results suggest that the PSGL1^{lo}CD4^{+} T cells have a PD1^{hi} CXCR5^{-} phenotype of extrafollicular B cell helpers.

PD1 deficiency in donor T cells leads to expansion of PSGL1^{lo}CD4^{+} T cells but reduction of autoantibody production

The role of PD1 expression by Tfh cells and its interaction with PD-L2 expression by B cells is known to be important during T-B interaction in GCs (6), but it remains unclear during extra-follicular T-B interaction, especially in non-lymphoid tissues. Therefore, we tested whether PD1 expressed by PSGL1^{lo}CD4^{+} T cells plays an important role in their interaction with B cells. Due to lack of mice with specific PD1 deficiency in T cells, we used PD1$^{-/-}$ C57BL/6 donors. Consistent with previous reports (27), PD1 deficiency in donor T cells markedly enhanced acute GVHD with different doses of donor spleen cells. The long-term survival was similar in recipients given 0.0625 x 10^6 PD1$^{-/-}$ donor Thy1.2^{+} T cells and in recipients given 0.25 x 10^6 WT donor Thy1.2^{+} T cells, and approximately half of the recipients survived up to 60 days in both groups with clinical signs of cGVHD such as weight-loss and hair-loss (Supplemental Figure 8A). Due to the different donor T cell doses, we did not focus on clinical cGVHD severity in the 2 groups. Instead, we focused on changes in histopathology and percentages of PSGL1^{lo}CD4^{+} T cells, naïve B, memory B, and plasma cells in the spleen and the liver tissues, as well as total IgG and anti-dsDNA IgG concentrations in the serum.

We observed that recipients given PD1$^{-/-}$ donor T cells had more lymphocyte infiltration in the liver tissue, but less damage in the skin and salivary gland, and no significant difference in the lung (Supplemental Figure 8B). The recipients given PD1$^{-/-}$ donor T cells also had less collagen deposition in the skin and salivary gland, although no obvious difference in the liver or lung

(Supplemental Figure 8C). Additionally, the recipients given PD1$^{-/-}$ T cells appeared to have less IgG deposition in the liver and skin tissues (Supplemental Figure 8D).

The yield of PSGL1^{lo}CD4^{+} T cells in the spleen and liver of recipients given PD1$^{-/-}$ donor T cells were higher as compared with recipients given WT donor T cells (Figure 4A). The CD19$^{lo/-}$ CD138^{+} plasma, CD19^{+}IgD^{+}CD80^{-} naïve B, and CD19^{+}IgD^{-}CD80^{+}PD-L2^{+} memory B cells were gated as shown in Supplemental Figure 8E. As compared with recipients given WT-T cells, the recipients given PD1$^{-/-}$ T cells had no significant difference in the percentage of naïve or memory B cells in the spleen and liver, but had a significant increase in the spleen and slight decrease in the percentage of CD19$^{lo/-}$CD138^{+} plasma cells in the liver (Figure 4B). In addition, the plasma cells in the spleen and liver of recipients given PD1$^{-/-}$ donor T cells had higher expression of Blimp-1 and IRF-4 (Supplemental Figure 8F), suggesting that they are IgG producing cells, as previously reported (28). Although total serum IgG concentrations were not different between the 2 groups, the serum concentrations of anti-dsDNA IgG were significantly lower in recipients given PD1$^{-/-}$ donor T cells (Figure 4C).

The lack of obvious reduction in the percentage of plasma cells in the liver of recipients given PD1$^{-/-}$ T cells might result from augmented GVHD induced by PD1$^{-/-}$ T cells. Consistent with this notion, the liver of recipients given PD1$^{-/-}$ TCD-BM alone contained higher percentages of memory B cells but lower percentages of plasma cells as compared with recipients given WT-TCD-BM alone (Supplemental Figure 8G). These results suggest that PD1 expression by PSGL1^{lo}CD4^{+} T cells is required for specific augmentation of anti-dsDNA IgG autoantibody production in cGVHD recipients. These results also suggest that PD1 expressed by PSGL1^{lo} CD4^{+} T cells may augment plasma cell expansion and autoantibody production in GVHD target tissues.

PD-L2 deficiency in donor B and other myeloid cells leads to expansion of PSGL1^{lo}CD4^{+} T cells but reduction of autoantibody production.

We also tested whether PSGL1^{lo}CD4^{+} T cell interaction with B cells requires expression of PD-L2 by B cells. Due to lack of mice with PD-L2 deficiency specific in B cells, we used PD-L2$^{-/-}$ C57BL/6 TCD-BM to provide PD-L2$^{-/-}$ B cells. WT-Thy1.2 (CD45.1^{+}, 0.25 x 10^{6}) were co-transplanted with TCD-BM (5 x 10^{6}) from WT (CD45.1^{+}) or PD-L2$^{-/-}$ (CD45.2^{+}) donors into lethal TBI-conditioned BALB/c recipients. As compared to recipients given WT-TCD-BM, recipients given PD-L2$^{-/-}$ TCD-BM showed slightly better survival (Supplemental Figure 9A). However, the recipients given PD-L2$^{-/-}$ TCD-BM cells showed less inflammation and damage in the lung, skin and salivary gland, although not in the liver. Collagen deposition in the lung, skin and salivary gland and IgG antibody deposition in the liver and skin were also lower in recipients given PD-L1$^{-/-}$ TCD-BM cells compared to those given WT cells (Supplemental Figure 9, B-D).

At 60 days after HCT, the percentage and yield of PSGL1^{lo}CD4^{+} T cells were higher in the liver tissues but not different in the spleen from recipients of PD-L2$^{-/-}$ BM as compared with WT BM (Figure 4D). The CD19$^{lo/-}$CD138^{+} plasma, CD19^{+}IgD^{+}CD80^{-} naïve B, and CD19^{+}IgD^{-}CD80^{+} CD73^{+} memory B cells were gated as shown in Supplemental Figure 8E and 9E. The percentages of naïve and memory B cells in the spleen and liver were not significantly different between the 2 groups, but plasma cells in the liver of recipient given PD-L2$^{-/-}$ BM were slightly reduced (Figure 4E). Both total IgG and anti-dsDNA IgG concentrations in the serum were significantly lower in the recipients of PD-L2$^{-/-}$ BM as compared with WT BM (Figure 4F). Interestingly, recipients given WT -T cells and WT or PD-L1$^{-/-}$ TCD-BM cells showed no significant difference in total serum IgG or anti-dsDNA-IgG concentrations, although the percentages of PSGL1^{lo}CD4^{+} T cells in the liver tissues were higher in recipients given PD-L1$^{-/-}$ BM as compared with WT BM (Supplemental Figure 10, A-C). These results suggest that PD-L2

but not PD-L1 expression by donor B cells is required to augment total IgG and anti-dsDNA IgG autoantibody production in cGVHD recipients.

PSGL1^{lo}CD4^{+} T cell interaction with B cells via PD1 and PD-L2 augments autoantibody production

In the experiments described above, PD-1 deficiency was not confined to PSGL1^{lo}CD4^{+} T cells and PD-L2 deficiency was not confined to B cells. Therefore, we used adoptive transfer experiments to determine whether PSGL1^{lo}CD4^{+} T cell PD1 interacts with B cell PD-L2 and regulates autoantibody production. As depicted in Figure 5A, sorted CD45.1^{+}PSGL1^{lo}CD4^{+} T cells and CD45.1^{+}PSGL1^{hi}CD4^{+} T cells (1x10^{6}) from the liver and lung of day 30 primary cGVHD recipients and sorted CD45.1^{+}PSGL1^{lo}CD4^{+} T cells from the spleen of GVHD-free recipients were injected into GVHD-free adoptive BALB/c chimeras grafted with donor-type C57BL/6 WT TCD-BM cells. Adoptive recipients given PBS were used as an additional control. At day 14 after cell transfer, the adoptive recipients were analyzed for the presence of the adoptively transferred CD45.1^{+} T cells in the spleen and liver, the percentage of plasma cells in the spleen and liver, and the serum concentration of total IgG and anti-dsDNA IgG.

The injected CD45.1^{+}PSGL1^{lo}CD4^{+} T and CD45.1^{+}PSGL1^{hi}CD4^{+} T cells were present in both the spleen and liver of the adoptive recipients, but they localized preferentially in the liver, especially with cells that originated from the liver and lung (Supplemental Figure 11 and Figure 5B). The numbers of CD45.1^{+} T cells recovered from spleen at day 14 after the adoptive transfer did not differ between recipients given non-GVHD or cGVHD PSGL1^{lo} cells or cGVHD PSGL1^{hi} cells. The numbers of CD45.1^{+} T cells recovered from the liver at day 14 after the adoptive transfer were more than 2-fold higher in recipients given cGVHD PSGL1^{lo}CD4^{+} T cells than in recipients given non-GVHD PSGL1^{lo}CD4^{+} T cells. The numbers of CD45.1^{+} T cells recovered from the liver did not differ between recipients given cGVHD PSGL1^{lo} or PSGL1^{hi} CD4^{+} T cells

(Figure 5B). These results indicate that PSGL1^{lo}CD4^{+} T and PSGL1^{hi}CD4^{+} T cells from cGVHD target tissues preferentially home back to the GVHD target tissues after transfer into adoptive recipients.

As compared to controls given PBS, injection of PSGL1^{lo}CD4^{+} T or PSGL1^{hi}CD4^{+} T cells did not change the percentage of plasma cells in the spleen of adoptive recipients. Injection of non-GVHD and cGVHD PSGL1^{lo}CD4^{+} T cells increased the percentage of plasma cells in the liver, while injection of cGVHD PSGL1^{hi}CD4^{+} T cells had no effect (Figure 5C). Similarly, injection of non-GVHD and cGVHD PSGL1^{lo}CD4^{+} T cells increased serum concentrations of total IgG and anti-dsDNA IgG, while injection of PSGL1^{hi}CD4^{+} T cells had no effect (Figure 5D). These results indicate that PSGL1^{lo}CD4^{+} T cells but not PSGL1^{hi}CD4^{+} T cells from cGVHD target tissues augment B cell differentiation to plasma cells and increase the production of IgG and anti-dsDNA autoantibodies.

To evaluate the role of PD-L2 expression by B cells interacting with PSGL1^{lo}CD4^{+} T cells, CD45.1^{+}PSGL1^{lo}CD4^{+} T cells from the liver and lung of primary cGVHD recipients were transferred into adoptive BALB/c chimeras grafted with C57BL/6 WT TCD-BM (WT chimeras) or PD-L2$^{-/-}$ TCD-BM (PD-L2$^{-/-}$ chimeras) (Figure 5E). The numbers of CD45.1^{+} T cells recovered from spleen at day 14 were lower in the PD-L2$^{-/-}$ chimeras than in WT chimeras, but the numbers of cells recovered from the liver did not show a statistically significant difference (Figure 5F). In WT chimeras, injection of PSGL1^{lo}CD4^{+} T cells increased the percentage of plasma cells in the liver and increased the serum concentrations of IgG and anti-dsDNA IgG. But in PD-L2$^{-/-}$ chimeras, injection of PSGL1^{lo}CD4^{+} T cells did not increase either the percentage of plasma cells or the serum concentrations of IgG or anti-dsDNA IgG (Figure 5, G and H). These results indicate that augmentation of B cell differentiation and IgG antibody production by PSGL1^{lo}CD4^{+} T cells requires B cell expression of PD-L2.

To evaluate the role of PD1 expression by PSGL1^{lo}CD4^{+} T cells, sorted WT or PD1$^{-/-}$ PSGL1^{lo} CD4^{+} T cells from the liver and lung of primary recipients were transferred into adoptive BALB/c chimeras grafted with C57BL/6 TCRβ$^{-/-}$TCD-BM cells (Figure 5I). The use of TCRβ$^{-/-}$TCD-BM was to avoid the influence of BM derived T cells. Again, the injected PSGL1^{lo}CD4^{+} T cells localized preferentially in the liver (Figure 5J). Injection of WT PSGL1^{lo}CD4^{+} T cells increased the percentage of plasma cells in the liver and increased the serum concentrations of IgG and anti-dsDNA-IgG. In contrast, injection of PD1$^{-/-}$ PSGL1^{lo}CD4^{+} T cells did not increase either the percentage of plasma cells or serum concentrations of IgG or anti-dsDNA IgG (Figure 5K and L). These results indicate that augmentation of B cell differentiation and IgG antibody production by PSGL1^{lo}CD4^{+} T cells in GVHD target tissues requires their expression of PD1.

To evaluate the PD1 and PD-L2 interaction between PSGL1^{lo}CD4^{+} T cells and B cells, we supplemented the in vivo results with in vitro culture experiments. Sorted CD19^{+}IgD^{+}CD80^{-} naïve B cells and CD19^{+}IgD^{-}CD80^{+}PD-L2^{+} memory B cells (2 - 5 x 10^4 cells/well) from the spleen of TCD-BM recipients were co-cultured with PSGL1^{lo}CD4^{+} T cells (0.4 – 1 x 10^4/well) from the liver and lung tissues of cGVHD recipients at 5:1 ratio for 4 days in the presence of anti-PD1, anti-PD-L2 or isotype control. PSGL1^{lo}CD4^{+} T cells augmented IgG production by memory B cells but not naïve B cells. The augmentation of IgG production by PSGL1^{lo}CD4^{+} T cells was blocked both by anti-PD1 and by anti-PD-L2 mAb (Supplemental Figure 12, A and B). These results indicate that PSGL1^{lo}CD4^{+} T cell augmentation of IgG production of memory B cells requires direct PD1 interaction with PD-L2.

Peripheral blood T cells give rise to PD1^{hi}PSGL1^{lo} Trm cells in murine cGVHD recipients. Since almost all CD4^{+} T cells among PBMC in donors and recipients were PSGL1^{hi}, with few PSGL1^{lo}CD4^{+} T cells (Figure 1 and Supplemental Figure 3), we tested whether murine PBMC

cells give rise to PSGL1^{lo}CD4^{+} Trm cells in GVHD target organs. PBMC (0.5x10^{6}, ~0.15-0.2x10^{6} T cells) and TCD-BM cells (5x10^{6}) from C57BL/6 donors were injected into lethal TBI-conditioned BALB/c mice. Recipients given TCD-BM alone were used as controls. The recipients given PBMC developed both acute and chronic GVHD as indicated by body weight-loss and some early deaths (Figure 6A). Recipients that survived for more than 60 days developed typical cGVHD histopathology in the liver, lung, skin and salivary gland (Figure 6B). As compared with GVHD-free recipients given TCD-BM alone, cGVHD recipients had higher percentages of PSGL1^{lo}CD4^{+} T cells in the spleen, liver and lung (Figure 6C), and most of them expressed high levels of PD1, ICOS and tissue-resident markers including CD69 and CXCR6 (Figure 6D). These results indicate that PSGL1^{hi}CD4^{+} T cells among PBMC can give rise to PSGL1^{lo}CD4^{+} T cells in GVHD target tissues of MHC-mismatched recipients.

PSGL1^{hi}CD4^{+} T cell differentiation into PSGL1^{lo}CD4^{+} T cells in cGVHD recipients is IL-6R-Stat3 pathway dependent

We previously reported that PSGL1^{lo}CD4^{+} T cell expansion in cGVHD recipients was Stat3-dependent (20), but it remains unknown whether PSGL1^{hi}CD4^{+} T differentiation into PSGL1^{lo} CD4^{+} T cells is also Stat3-dependent. To answer this question, we transplanted PBMC containing nearly 100% PSGL1^{hi} T cells (0.5x10^{6}, ~0.15-0.20x10^{6} T cells) from CD45.2^{+} WT or Stat3$^{-/-}$ donors together with CD45.1^{+} TCD-BM cells (5x10^{6}) from WT donors into lethal TBI conditioned BALB/c recipients. The recipients given PBMC from WT donors developed acute and chronic GVHD with weight-loss and ~70% (10/15) survived for more than 40 days; in contrast, the recipients given PBMC from Stat3$^{-/-}$ PBMC showed little signs of GVHD and 100%(10/10) survived for more than 40 days (Figure 7A). The percentages of PSGL^{lo}CD4^{+} T cells among the injected CD45.2^{+} donor T cells in the spleen, liver and lung at 40 days after HCT were lower with Stat3$^{-/-}$ T cells than with WT T cells (Fig. 7B). These results indicate that Stat3 promotes the differentiation of PSGL1^{hi}CD4^{+} T cells into PSGL1^{lo}CD4^{+} T cells.

IL-6R signaling activates Stat3 signaling pathway (29). Blockade of IL-6R signaling by anti-IL6R mAbs ameliorates GVHD in murine models and in humans with concomitant expansion of Treg cells (30, 31). We tested whether blockade of IL-6R signaling by anti-IL-6R could regulate $PSGL1^{hi}CD4^{+}$ T differentiation into $PSGL1^{lo}CD4^{+}$ T cells. Accordingly, lethal TBI-conditioned BALB/c recipients were grafted with $CD45.2^{+}$ PBMC and $CD45.1^{+}$ TCD-BM. The recipients were treated with anti-IL6R mAb or control rat IgG (500 µg/mouse) from days-1 and 0 and then weekly for 4 weeks. Anti-IL-6R mAb treatment reduced the severity of GVHD as indicated by lower loss of body weight (Figure 7C). Anti-IL6R treatment also significantly reduced the percentage of $PSGL1^{lo}CD4^{+}$ T cells among the injected donor $CD4^{+}$ T cells in the liver and lung, but not in the spleen (Figure 7D). Taken together, these results show that the IL-6R-Stat3 signaling pathway promotes $PSGL1^{hi}CD4^{+}$ T differentiation into $PSGL^{1o}CD4^{+}$ T cells in cGVHD target tissues.

Human peripheral blood T cells give rise to $PD1^{hi}PSGL1^{lo}CD4^{+}$ Trm cells that interact with B cells in the GVHD target tissues in humanized recipients

We tested whether human $PSGL1^{hi}CD4^{+}$ T cells gave rise to $PSGL1^{lo}CD4^{+}$ T cells using a humanized murine model, in which MHC-I and II deficient ($MHC^{-/-}$) NSG mice that express human HLA-A2 and HLA-DR4 ($A2^{+}DR4^{+}$ NSG) were used as recipients, and HLA-$A2^{-}DR4^{-}$ healthy volunteers were used as donors. $A2^{-}DR4^{-}$ PBMC containing $12x10^{6}$ T cells were injected into $MHC^{-/-}$HLA-$A2^{+}DR4^{+}$ NSG recipients or control $MHC^{-/-}$ NSG recipients. While $MHC^{-/-}$ NSG recipients showed little signs of GVHD and appeared to be healthy, the $A2^{+}DR4^{+}$ NSG recipients developed severe GVHD with bodyweight loss, hair-loss, although they all survived for more than 60 days (Figure 8A). The HLA-$A2^{+}DR4^{+}$ cGVHD recipients showed inflammatory infiltration, human IgG deposition, collagen deposition in the liver, lung, skin and salivary glands, and high serum concentrations of anti-dsDNA human IgG. In contrast, $MHC^{-/-}$ recipients showed

some infiltration but little human IgG or collagen deposition in the tissues and low serum concentrations of anti-dsDNA human IgG (Figure 8,B-D; and Supplemental Figure13A). These results indicate that HLA-A2^{-}DR4^{-} human PBMC can induce autoimmune-like cGVHD in humanized MHC$^{-/-}$HLA-A2^{+}DR4^{+} NSG recipients.

PSGL1^{lo}CD4^{+} T cells were not present among PBMC of A2^{+}DR4^{+} NSG recipients with cGVHD, but 10-20% of PSGL1^{lo}CD4^{+} T cells were present among donor CD4^{+} T cells in the spleen, liver and lung (Figure 8E), and most of them expressed markers of Trm, including high expression of CD69 and low expression of CCR7, with no difference in CD103 expression, as compared with PSGL1^{hi}CD4^{+} T cells (Figure 8F). In addition, the PSGL1^{lo}CD4^{+} T cells have high expression of PD1, ICOS and TIGIT, but not CXCR5 (Figure 8G). Finally, the PSGL1^{lo}CD4^{+} T cells in the liver produced IFN-γ and IL-21 and expressed CD40L (Supplemental Figure 13B). Taken together, these results indicate that PSGL1^{lo}CD4^{+} T cells derived from human peripheral blood T cells in GVHD target tissues of a humanized murine model are tissue-resident T cells with B cell helper potential.

Human PSGL1^{lo}CD4^{+} T cells augment autologous memory B cell differentiation into plasma cells in a PD1/PD-L2-dependent manner.

To evaluate whether experiments with murine cells are relevant for human cells, we tested whether the PSGL1^{lo}CD4^{+} T cells interact with B cells in humanized NSG recipients given whole human PBMC containing ~12% CD19^{+} B cells and ~45% T cells (Supplemental Figure 14A). At day 60, donor B cells were hardly detectable in the blood, liver or lung tissues of control MHC$^{-/-}$ NSG recipients. Only ~0.5% CD19^{+} B cells were detected among splenic mononuclear cells (MNC), and most of them were CD27^{-}CD38^{-} “naïve” B cells (Supplemental Figure 14B). On the other hand, CD19^{+} B cells could be detectable in the blood, spleen, liver and lung tissues of HLA-A2^{+}DR4^{+} humanized NSG recipients with cGVHD. In the blood, ~80% of the B cells had a

$CD27^-CD38^-$ "naïve" phenotype, ~20% had a $CD27^+CD38^-$ memory B phenotype, and none had a $CD27^+CD38^+$ plasmablast phenotype. In contrast, B cells in the spleen, liver and lung contained 25-50% $CD27^+CD38^-$ memory B cells and 6-8% $CD27^+CD38^+$ plasmablasts (Supplemental Figure 14C). These results indicate that human B cells are activated and expanded in humanized $A2^+DR4^+$ NSG mice with cGVHD.

To evaluate the interaction between $PSGL1^{lo}CD4^+$ T and B cells in GVHD target tissues of humanized recipients, we used adjacent slides of formalin-fixed liver tissues to identify $PSGL1^{lo}$ $CD4^+$ T cells and memory B cells, by combination histoimmunochemistry staining of 1) Maf (T cell marker), CD4 and CD20; 2) Maf, PSGL1 and PAX5 (B cell marker); 3) CD4, PAX5, CD27 (marker for memory B and $CD4^+$ T) (Figure 9A). Since we observed that, like other B cell helpers, $PSGL1^{lo}CD4^+$ T cells expressed higher levels of MAF (Figure 3E), we calculated the numbers of MAF^+CD4^+ or $MAF^+PSGL1^{lo/-}$ T cells that were juxtaposed with B cells. The numbers of MAF^+CD4^+ T cells co-localizing with $CD20^+$ B cells and the numbers of $MAF^+PSGL1^{lo/-}$ T cells co-localizing with $PAX5^+PSGL1^+$ B cells in the tissue were markedly higher than in control $MHC^{-/-}$ NSG recipients without cGVHD (Figure 9B). This is also consistent with flow cytometry analysis that many donor B cells were present in the liver of humanized cGVHD mice but few donor B cells were present in the liver of control mice (Supplemental Figure 14, B and C). Taken together, human $PSGL1^{lo}CD4^+$ T cells-derived from PBMC $PSGL1^{hi}CD4^+$ T cells interact with memory B cells in the liver tissue of humanized cGVHD recipients.

To directly evaluate the interactions of human $PSGL1^{lo}CD4^+$ T cells with autologous B cells, sorted human $PSGL1^{lo}CD4^+$ T cells from GVHD target tissues including spleen, liver and lung of humanized HLA-$A2^+DR4^+$ NSG mice were co-cultured in vitro with sorted $CD3^-CD19^+CD38^{lo/-}$ $CD27^-$ naïve or $CD3^-CD19^+CD38^-CD27^+$ memory B cells from the same human PBMC that were cryopreserved in liquid nitrogen when we performed the primary transfer experiments. Sorting of

naïve and memory B cells is depicted in (Supplemental Figure 15A). PSGL1^{lo}CD4^{+} T cells did not augment naïve B cell differentiation into CD138^{+}CD27^{+} plasma cells (Figure 9C). In contrast, PSGL1^{lo}CD4^{+} T cells significantly augmented memory B cell differentiation into CD27^{+}CD138^{+} plasma cells (Figure 9D). Besides augmenting plasma cell expansion, PSGL1^{lo}CD4^{+} T cells also augmented IgG production, and the effect was blocked by IL-21R Fc (Figure 9E). Finally, blocking anti-PD1 and anti-PD-L2 markedly reduced the yield of plasma cells in the culture (Figure 9F). As compared with naïve B cells, human memory B cells express high levels of PD-L2 as indicated by MFI PD-L2 (Supplemental Figure 15B). These results indicate that human PSGL1^{lo}CD4^{+} T cells from GVHD target tissues of humanized murine recipients can augment autologous memory B cell differentiation into plasma cells and augment their antibody production in a PD1- and PD-L2-dependent manner.

PDGL1^{lo}CD4^{+} T cells appear to interact with memory B cells in GVHD target tissues of cGVHD patients.

Next, we attempted to link our studies of PSGL1^{lo}CD4^{+} T interaction with B cells in the mouse model and humanized mouse model to patients with cGVHD. Consistent with our studies with mouse and humanized mouse models (Figure 1 and 8), PSGL1^{lo}CD4^{+} T cells were undetectable among PBMC of healthy human donors or cGVHD patients (Figure 10, A and B). Because we observed PSGL1^{lo}CD4^{+} T and memory B interactions in the liver tissue of mouse and humanized mouse cGVHD recipients (Figure 2; and Figure 9, A and B), we tested whether similar interactions exist in the liver tissue of cGVHD patients.

Similar to histoimmunochemistry staining with formalin-fixed tissues in Figure 9A, we used 4 adjacent sections with staining combinations of 1) MAF (T cell marker), CD3, and CD20; 2) MAF, CD4 and CD20; 3) MAF, PSGL1, and PAX5 (B cell marker); 4) CD3, PAX5, and CD27 (marker for memory B and CD4^{+} T cells) (Figure 10C). As mentioned in Figure 9, we used MAF staining

to identify the potential PSGL1^{lo}CD4^{+} T cells of B cell helper. We observed that there were many T and B cells in the tissues (Figure 10C). We calculated the percentage of MAF^{+} T cells that were juxtaposed with PAX5^{+} B cells, and approximately 60-80% MAF^{+} T cells were CD3^{+}, CD4^{+}, or PSGL1$^{lo/-}$, and ~20% PAX5^{+} B cells were CD27^{+} memory B cells (Figure 10D). These observations suggest that an interaction between PSGL1$^{lo/-}$CD4^{+} T cells and memory B cells exists in the liver tissue of cGVHD patients.

Discussion

Extrafollicular PSGL1^{lo}CD4^{+} T cells that help B cell production of autoantibodies in lymphoid tissue of autoimmune SLE mice were identified more than a decade ago by Craft et al. (9). We recently showed that PSGL1^{lo}CD4^{+} T cells are expanded in GVHD target tissues of autoimmune-like cGVHD mouse recipients that had destruction of lymphoid follicles (20). However, PSGL1^{lo}CD4^{+} T cells in humans have not been reported, and the function of PSGL1^{lo} CD4^{+} T cells in non-lymphoid tissues remained unclear. Using a murine model of cGVHD that emerges from aGVHD (16) together with a humanized MHC$^{-/-}$HLA-A2^{+}DR4^{+} cGVHD model, we have demonstrated that both mouse and human PSGL1^{lo}CD4^{+} T cells in GVHD target tissues are PD1^{hi} tissue-resident B cell helpers that augment memory B cell differentiation into antibody producing plasma cells through their PD1 interaction with PD-L2 on B cells. The extrafollicular PD1^{hi} PSGL1^{lo} B cell helpers from GVHD target tissues preferentially augment autoantibody production.

PD1^{hi}PSGL1^{lo}CD4^{+} T cells from GVHD target tissues are pathogenic tissue-resident B cell helpers. High PD1 expression can indicate anergy or exhaustion, as is the case for PD1^{+} Eomes^{+} T cells in target tissues of aGVHD (32), and PD1 deficiency in donor T cells exacerbates aGVHD (27). Other results, however, have shown that alloreactive T cells with upregulated expression of PD1 alone in GVHD patients are not anergic/exhausted (26). Consistently, both murine and human PD1^{hi}PSGL1^{lo}CD4^{+} T cells from GVHD target tissues down-regulated expression of anergy markers TIM 3 and LAG3, upregulated expression of B cell helper markers of ICOS and IL-21, and upregulated expression of tissue-resident receptors CD69, CXCR6, and P2RX7. Our adoptive transfer and ex vivo coculture experiments showed that sorted murine and human PSGL1^{lo}CD4^{+} T cells from GVHD target tissues augmented memory B cell differentiation into antibody-producing plasma cells in a manner that depends on

PD1 interaction with PD-L2. Taken collectively, we have demonstrated that murine and human PSGL1^{lo}CD4^{+} T cells are tissue-resident B cell helpers that do not circulate in the blood. They differ from PD1^{hi}CXCR5^{-} B cell helpers identified in human RA synovial fluid, a population that can circulate in the blood (33). They also differ from extrafollicular CXCR5^{-}CXCR4^{+}PSGL1^{lo} CD4^{+} T cells in the spleen of SLE mice (9), because they lack expression of CXCR4. The transcriptional regulation of the PD1^{hi}PSGL1^{lo}CD4^{+} Trm cell differentiation has not been fully defined. CD8^{+} Trm cell differentiation in mice infected by Herpes Simplex virus (HSV) is synergistically controlled by Hobit and Blimp 1 (34). Similarly, CD4^{+} Trm cell differentiation and their production of proinflammatory cytokines and chemokines is synergistically regulated by Hobit and Blimp1 (35). CD8^{+} Trm cells shape local and systemic secondary T cell responses, and Hobit^{+}CD8^{+} Trm cells can give rise to circulating memory T cells that do not express Hobit (36). In RNA-seq analysis, we found that neither PSGL1^{lo} nor PSGL1^{hi} CD4^{+} T cells from GVHD target tissues expressed detectable levels of Hobit, but they both expressed Blimp1, with no significant difference between them. Therefore, the transcriptional regulation of Trm cells in GVHD target tissues may differ from those in viral infection or autoimmune colitis (35). The role of Hobit, Blimp1 and other transcriptional factors in regulating CD4^{+} Trm formation in GVHD target tissues is under investigation.

IgG autoantibodies produced by memory B cells that interact with PSGL1^{lo}CD4^{+} T cells may augment fibrosis in GVHD target tissues. We observed that the presence of human PD1^{hi} PSGL1^{lo}CD4^{+} T cells, memory B cells and IgG antibody deposition in the humanized NSG mice were associated with markedly enhanced fibrosis in the GVHD target tissues. This is consistent with reports that anti-PDGFR and anti-cell membrane antigen autoantibodies augment cGVHD in patients (37, 38). Other factors may also contribute to the fibrosis, because PSGL1^{lo}CD4^{+} T cells produce IL-17 in addition to IL-21, IL-13 and IFN-γ (20). PD1^{+}IL-17-producing CD4^{+} T cells mediated fibrosis in the lung (39).

Alloreactive $CD4^+$ T-derived autoreactive $PSGL1^{lo}CD4^+$ T cell interaction with B cells in GVHD target tissues augments expansion of autoreactive B cells, leading to increased autoantibody production. HLA-$A2^{-/-}DR4^{-/-}$ human PBMC showed little expansion of B cells or little increase of serum anti-dsDNA human IgG in $MHC^{-/-}$ NSG recipients, but they showed expansion of memory B and plasma cells and high-level serum anti-dsDNA human IgG in $MHC^{-/-}A2^+DR4^+$ NSG recipients, indicating that alloreactive $CD4^+$ T cells from human PBMC can become autoreactive $CD4^+$ T cells in GVHD recipients and activate autologous autoreactive B cells to produce autoantibodies. This is consisting with our previous report in mouse models that alloreactive $CD4^+$ T cells become autoreactive T cells in cGVHD recipients (12). In addition, we found that the autoantibody production in cGVHD recipients was dependent on $PSGL1^{lo}CD4^+$ T cell PD1 interaction with PD-L2 on B cells in mouse models. This may result from that PD-$L2^{hi}$ B cells in different tissues present different antigens to expand different autoreactive $PD1^{hi}PSGL1^{lo}CD4^+$ T cell clones. Our previous studies showed that $CD4^+$ T and B interactions led to clonal expansion of autoreactive $CD4^+$ T cells in cGVHD recipients (3).

Extrafollicular $PSGL1^{lo}CD4^+$ T cell interaction with B cells differs from $PD1^{hi}$Tfh interaction with B cells in the germinal center. $PD1^{hi}$Tfh interaction with GC B cells via PD1/PD-L2 was proposed to mediate negative selection of autoreactive $CD4^+$ Tfh cells, in addition to regulating GC B cell affinity maturation and formation of long-lived plasma cells (6, 40). The presence of extrafollicular autoreactive $PD1^{hi}CD4^+$ T cells including $PD1^{hi}CXCR5^-$ Tfh-like cells in RA synovial tissues (33) and $PD1^{hi}CXCR5^-PSGL1^{lo}CD4^+$ T cells in the target tissues of cGVHD described in the current studies may indicate a lack of negative selection against autoreactive $PD1^{hi}CD4^+$ T cells during T-B interaction in the inflammatory non-lymphoid tissues.

Autoreactive PD1^{hi}PSGL1^{lo}CD4^{+} T cells may be derived from anergic/exhausted autoreactive T cells among PSGL1^{hi}CD4^{+} T cells in the donor PBMC. Autoreactive T cells are present in the periphery of healthy individuals, often with anergic or exhausted phenotype (41), but they can be revived by lymphopenia or by exposure to inflammation (42-44). Consistently, we observed although all CD4^{+} T cells in murine or human PBMC were PSGL1^{hi} before HCT, both gave rise to PD1^{hi}PSGL1^{lo}CD4^{+} T cells in GVHD target tissues of recipient mice. Development of PD1^{hi} PSGL1^{lo}CD4^{+} T cells in mice depends on IL-6R-Stat3 signaling. Our observations could explain why infusion of G-CSF-mobilized blood grafts containing more donor T cells cause more severe autoimmune-like cGVHD, even though the severity of aGVHD was reduced (45, 46). Higher numbers of T cells in the graft may lead to more abundant autoreactive PD1^{hi}PSGL1^{lo}CD4^{+} T cells that can augment the autoantibody production that worsens tissue damage.

PD1^{hi}PSGL1^{lo}CD4^{+} T cell interaction with B cells indirectly augments cutaneous cGVHD pathogenesis by augmenting antibody production outside skin tissues. We reported that donor B cells contribute to cGVHD pathogenesis through their APC function that expand pathogenic CD4^{+} T cells as well as their production of antibodies. IgG antibodies from donor B cells were not required to initiate cGVHD but were required for the persistence of cutaneous GVHD (3, 4). In the current studies, we found that donor-type B cells and PD1^{hi}PSGL1^{lo}CD4^{+} B cell helpers were nearly undetectable in the skin tissue of cGVHD mice and humanized cGVHD mice, although both PD1^{hi}PSGL1^{lo}CD4^{+} T cells and B cells were present in the liver and lung. We observed IgG deposition and fibrosis in the GVHD target tissues of humanized mice with expansion of donor-type B in the liver and lung but not in control mice without expansion of donor-type B cells. Therefore, we propose that cutaneous fibrosis results from deposition of autoantibodies produced by B-lineage cells located in other tissues such as the liver and lung.

We believe that targeting tissue-resident T cells may represent a novel approach for preventing and treating autoimmune-like cGVHD and other autoimmune diseases. In preclinical models, therapy with depleting anti-CD20 prevented autoimmune cGVHD and other autoimmune diseases but did not effectively treat ongoing cGVHD or autoimmune diseases, because expression of CD20 was lost by activated B cells in the tissue (47, 48). Blockade of BCR signaling by the BTK inhibitor Ibrutinib is effective in some patients with cGVHD and other autoimmune diseases (49, 50). Therefore, targeting B cells alone does not control autoimmune diseases or chronic GVHD in all cases. Administration of NAD that targets P2RX7 and augments apoptosis of Trm cells ameliorated colitis (35). It would be of interest to test whether targeting PSGL1^{lo}CD4^{+} Trm cells by NAD is effective for autoimmune diseases that do not improve after treatment with B cell-specific agents.

In summary, the current studies have unraveled new insights into T-B interactions in the non-lymphoid target tissues of cGVHD recipients. We propose that, as depicted in the diagram (Figure 11), donor-type alloreactive PSGL1^{hi}CD4^{+} T cells from donor graft interact with host-type APCs in the lymphoid tissues and become activated PD1^{hi}PSGL1^{lo}CD4^{+} autoreactive T cells that recognize autoantigens presented by donor B cells. This interaction leads to activation of autoreactive B cells and production of IgG antibodies that augment damage in lymphoid tissues, resulting in lymphopenia, as described in our previous publication (20). In the GVHD target tissues, the PD1^{hi}PSGL1^{lo}CD4^{+} T cells differentiate into tissue-resident T cells with high expression of CD69, CXCR6, and P2RX7 in an IL-6R/Stat3 dependent manner. These cells may attract donor-type activated/memory B cells into the target tissues. At the same time, those PD1^{hi}PSGL1^{lo}CD4^{+} autoreactive T cells recognize autoantigens presented by the donor B cells and interact with the B cells via TCR-MHC complex and other co-stimulatory molecules including PD1 and PD-L2. The interactions of T cell PD1 with B cell PD-L2 leads to enhanced production of IgG autoantibodies that augment tissue damage. Circulating IgG autoantibodies

also deposited in the skin to augment skin GVHD, although neither PSGL1^{lo}CD4^{+} T nor B cells infiltrate the skin. Our data indicate that PSGL1^{hi}CD4^{+} T cells can contribute to autoantibody-mediated cGVHD pathogenesis only by becoming PSGL1^{lo}CD4^{+} cells that acquire B cell helper function. The extent to which PSGL1^{hi}CD4^{+} T cells contribute to the pathogenesis of cGVHD through autoantibody-independent mechanisms remains to be determined.

Materials and Methods

Mice:

BALB/c and C57BL/6 mice were purchased from National Cancer Institute Laboratories. PD1$^{-/-}$ and PD-L1$^{-/-}$ C57BL/6 breeders were provided by Dr. Haidong Dong (Mayo Clinic, Rochester, Minnesota) with approval of Dr. Honjo, Tokyo University. Spleen and bone marrow from PD-L2$^{-/-}$ C57BL/6 mice were provided by Dr. Karen M. Hass (Wake Forest University, Winston-Salem, North Carolina). MHC$^{-/-}$ NSG and MHC$^{-/-}$HLA-A2^{+}DR4^{+} mice were established by backcrossing β2m$^{-/-}$ MHC-II$^{-/-}$ NSG mice with HLA-A2^{+} or DR4^{+} NSG mice purchased from the Jackson laboratory at Research Animal Center (ARC) of City of Hope (COH).

GVHD patients and healthy donor information:

The patients' information including gender, age, disease, graft type, conditioning, GVHD prophylaxis and GVHD grade are detailed in Supplementary Table 1. Control subjects are detailed in Supplementary Table 2.

Experimental procedures:

Experimental procedures including 1) induction and assessment of GVHD; 2) isolation of lymphocytes from GVHD target tissues; 3) antibodies, flow cytometry analysis and cell sorting; 5) histopathology, histoimmunochemistry and histoimmunofluorescent staining; 6) tissue IgG deposition; 7) RNA sequencing analysis; 8) ELISA of total IgG and anti-dsDNA IgG; 9) adoptive cell transfer; 9) T-B cells co-cultures have been described in previous publications (3, 4, 12, 16, 20, 33) and supplemental methods.

Data availability:

The RNA sequencing data have been deposited and available in the GEO database: GSE157566.

Statistical analysis:

Data were shown as mean ± SEM. Comparison of %Survival in groups was analyzed by log-rank test. Two group means comparison was analyzed by using an unpaired two-tailed Student t-test. For evaluation of three means, we use one-way ANOVA multiple comparisons (Prism version 7). P-values less than 0.05 were considered to be statistically significant.

Study approval:

All mice were kept in a specific pathogen-free room in COH-ARC, and all animal protocols were approved by the City of Hope Institutional Animal Care and Use Committee (IACUC). All subjects gave written informed consent according to protocols approved under COH IRB file 15172.

Author Contributions: XK designed, performed research, acquired and analyzed data, and prepared the manuscript. XW and HQ performed RNA-sequencing and data analysis. DYZ designed and performed research and acquired data. MS, BW performed immunofluorescent staining. SY, QS, YZ, MS, UN assisted in experiments. KMH provided PD-L2$^{-/-}$ C57BL/6 mice and critical review the manuscript. ADR provided advice for RNA-sequencing analysis, reviewed manuscript and provided financial support for this project. RN provided advice on human related studies, organized human samples, and reviewed the manuscript. PJM provided advice on experimental design and critical review and editing manuscript. AH is DYZ' PhD advisor. DFZ designed and supervised the research and wrote the manuscript.

***Funding**:* This work was supported by National Institutes of Health Grant R01 AI066008 and R01 CA228465 (to D. Zeng), as well as supported by Legacy Heritage Fund and NCI P30CA033572.

References:

1. Seth A, and Craft J. Spatial and functional heterogeneity of follicular helper T cells in autoimmunity. *Curr Opin Immunol.* 2019;61:1-9.
2. Zhang C, Todorov I, Zhang Z, Liu Y, Kandeel F, Forman S, Strober S, and Zeng D. Donor CD4+ T and B cells in transplants induce chronic graft-versus-host disease with autoimmune manifestations. *Blood.* 2006;107(7):2993-3001.
3. Young JS, Wu T, Chen Y, Zhao D, Liu H, Yi T, Johnston H, Racine J, Li X, Wang A, et al. Donor B cells in transplants augment clonal expansion and survival of pathogenic CD4+ T cells that mediate autoimmune-like chronic graft-versus-host disease. *J Immunol.* 2012;189(1):222-33.
4. Jin H, Ni X, Deng R, Song Q, Young J, Cassady K, Zhang M, Forman S, Martin PJ, Liu Q, et al. Antibodies from donor B cells perpetuate cutaneous chronic graft-versus-host disease in mice. *Blood.* 2016;127(18):2249-60.
5. Crotty S. T Follicular Helper Cell Biology: A Decade of Discovery and Diseases. *Immunity.* 2019;50(5):1132-48.
6. Good-Jacobson KL, Szumilas CG, Chen L, Sharpe AH, Tomayko MM, and Shlomchik MJ. PD-1 regulates germinal center B cell survival and the formation and affinity of long-lived plasma cells. *Nat Immunol.* 2010;11(6):535-42.
7. Freeman GJ, Long AJ, Iwai Y, Bourque K, Chernova T, Nishimura H, Fitz LJ, Malenkovich N, Okazaki T, Byrne MC, et al. Engagement of the PD-1 immunoinhibitory receptor by a novel B7 family member leads to negative regulation of lymphocyte activation. *J Exp Med.* 2000;192(7):1027-34.
8. Somers WS, Tang J, Shaw GD, and Camphausen RT. Insights into the molecular basis of leukocyte tethering and rolling revealed by structures of P- and E-selectin bound to SLe(X) and PSGL-1. *Cell.* 2000;103(3):467-79.
9. Odegard JM, Marks BR, DiPlacido LD, Poholek AC, Kono DH, Dong C, Flavell RA, and Craft J. ICOS-dependent extrafollicular helper T cells elicit IgG production via IL-21 in systemic autoimmunity. *J Exp Med.* 2008;205(12):2873-86.
10. Ferrara JL, Levine JE, Reddy P, and Holler E. Graft-versus-host disease. *Lancet.* 2009;373(9674):1550-61.
11. Zeiser R, and Blazar BR. Pathophysiology of Chronic Graft-versus-Host Disease and Therapeutic Targets. *New Engl J Med.* 2017;377(26):2565-79.
12. Zhao D, Young JS, Chen YH, Shen E, Yi T, Todorov I, Chu PG, Forman SJ, and Zeng D. Alloimmune response results in expansion of autoreactive donor CD4+ T cells in transplants that can mediate chronic graft-versus-host disease. *J Immunol.* 2011;186(2):856-68.
13. Tivol E, Komorowski R, and Drobyski WR. Emergent autoimmunity in graft-versus-host disease. *Blood.* 2005;105(12):4885-91.
14. Bleakley M, Heimfeld S, Loeb KR, Jones LA, Chaney C, Seropian S, Gooley TA, Sommermeyer F, Riddell SR, and Shlomchik WD. Outcomes of acute leukemia patients transplanted with naive T cell-depleted stem cell grafts. *J Clin Invest.* 2015;125(7):2677-89.
15. Zhang Y, Hexner E, Frank D, and Emerson SG. CD4+ T cells generated de novo from donor hemopoietic stem cells mediate the evolution from acute to chronic graft-versus-host disease. *J Immunol.* 2007;179(5):3305-14.
16. Wu T, Young JS, Johnston H, Ni X, Deng R, Racine J, Wang M, Wang A, Todorov I, Wang J, et al. Thymic damage, impaired negative selection, and development of chronic graft-versus-host disease caused by donor CD4+ and CD8+ T cells. *J Immunol.* 2013;191(1):488-99.

17. Sarantopoulos S, and Ritz J. Aberrant B-cell homeostasis in chronic GVHD. *Blood.* 2015;125(11):1703-7.
18. Radojcic V, Pletneva MA, Yen HR, Ivcevic S, Panoskaltsis-Mortari A, Gilliam AC, Drake CG, Blazar BR, and Luznik L. STAT3 signaling in CD4+ T cells is critical for the pathogenesis of chronic sclerodermatous graft-versus-host disease in a murine model. *J Immunol.* 2010;184(2):764-74.
19. Flynn R, Du J, Veenstra RG, Reichenbach DK, Panoskaltsis-Mortari A, Taylor PA, Freeman GJ, Serody JS, Murphy WJ, Munn DH, et al. Increased T follicular helper cells and germinal center B cells are required for cGVHD and bronchiolitis obliterans. *Blood.* 2014;123(25):3988-98.
20. Deng R, Hurtz C, Song Q, Yue C, Xiao G, Yu H, Wu X, Muschen M, Forman S, Martin PJ, et al. Extrafollicular CD4(+) T-B interactions are sufficient for inducing autoimmune-like chronic graft-versus-host disease. *Nat Commun.* 2017;8(1):978.
21. Masopust D, and Soerens AG. Tissue-Resident T Cells and Other Resident Leukocytes. *Annu Rev Immunol.* 2019;37(521-46.
22. Mueller SN, and Mackay LK. Tissue-resident memory T cells: local specialists in immune defence. *Nat Rev Immunol.* 2016;16(2):79-89.
23. Oh JE, Iijima N, Song E, Lu P, Klein J, Jiang R, Kleinstein SH, and Iwasaki A. Migrant memory B cells secrete luminal antibody in the vagina. *Nature.* 2019;571(7763):122-6.
24. Schroeder MA, and DiPersio JF. Mouse models of graft-versus-host disease: advances and limitations. *Dis Model Mech.* 2011;4(3):318-33.
25. Yi T, Chen Y, Wang L, Du G, Huang D, Zhao D, Johnston H, Young J, Todorov I, Umetsu D, et al. Reciprocal differentiation and tissue-specific pathogenesis of Th1, Th2, and Th17 cells in graft versus host disease. *Blood.* 2009;114(14):3101-12.
26. Simonetta F, Pradier A, Bosshard C, Masouridi-Levrat S, Dantin C, Koutsi A, Tirefort Y, Roosnek E, and Chalandon Y. Dynamics of Expression of Programmed Cell Death Protein-1 (PD-1) on T Cells After Allogeneic Hematopoietic Stem Cell Transplantation. *Front Immunol.* 2019;10:1034.
27. Blazar BR, Carreno BM, Panoskaltsis-Mortari A, Carter L, Iwai Y, Yagita H, Nishimura H, and Taylor PA. Blockade of programmed death-1 engagement accelerates graft-versus-host disease lethality by an IFN-gamma-dependent mechanism. *J Immunol.* 2003;171(3):1272-7.
28. Shapiro-Shelef M, and Calame K. Regulation of plasma-cell development. *Nat Rev Immunol.* 2005;5(3):230-42.
29. Yu H, Pardoll D, and Jove R. STATs in cancer inflammation and immunity: a leading role for STAT3. *Nat Rev Cancer.* 2009;9(11):798-809.
30. Chen X, Das R, Komorowski R, Beres A, Hessner MJ, Mihara M, and Drobyski WR. Blockade of interleukin-6 signaling augments regulatory T-cell reconstitution and attenuates the severity of graft-versus-host disease. *Blood.* 2009;114(4):891-900.
31. Kennedy GA, Varelias A, Vuckovic S, Le Texier L, Gartlan KH, Zhang P, Thomas G, Anderson L, Boyle G, Cloonan N, et al. Addition of interleukin-6 inhibition with tocilizumab to standard graft-versus-host disease prophylaxis after allogeneic stem-cell transplantation: a phase 1/2 trial. *Lancet Oncol.* 2014;15(13):1451-9.
32. Ni X, Song Q, Cassady K, Deng R, Jin H, Zhang M, Dong H, Forman S, Martin PJ, Chen YZ, et al. PD-L1 interacts with CD80 to regulate graft-versus-leukemia activity of donor CD8+ T cells. *J Clin Invest.* 2017;127(5):1960-77.
33. Rao DA, Gurish MF, Marshall JL, Slowikowski K, Fonseka CY, Liu Y, Donlin LT, Henderson LA, Wei K, Mizoguchi F, et al. Pathologically expanded peripheral T helper cell subset drives B cells in rheumatoid arthritis. *Nature.* 2017;542(7639):110-4.
34. Mackay LK, Minnich M, Kragten NA, Liao Y, Nota B, Seillet C, Zaid A, Man K, Preston S, Freestone D, et al. Hobit and Blimp1 instruct a universal transcriptional program of tissue residency in lymphocytes. *Science.* 2016;352(6284):459-63.
35. Zundler S, Becker E, Spocinska M, Slawik M, Parga-Vidal L, Stark R, Wiendl M, Atreya R, Rath T, Leppkes M, et al. Hobit- and Blimp-1-driven CD4(+) tissue-resident memory T cells control chronic intestinal inflammation. *Nat Immunol.* 2019;20(3):288-300.
36. Behr FM, Parga-Vidal L, Kragten NAM, van Dam TJP, Wesselink TH, Sheridan BS, Arens R, van Lier RAW, Stark R, and van Gisbergen K. Tissue-resident memory CD8(+) T cells shape local and systemic secondary T cell responses. *Nat Immunol.* 2020;21(9):1070-81.
37. Wang KS, Kim HT, Nikiforow S, Heubeck AT, Ho VT, Koreth J, Alyea EP, Armand P, Blazar BR, Soiffer RJ, et al. Antibodies targeting surface membrane antigens in patients with chronic graft-versus-host disease. *Blood.* 2017;130(26):2889-99.

38. Svegliati S, Olivieri A, Campelli N, Luchetti M, Poloni A, Trappolini S, Moroncini G, Bacigalupo A, Leoni P, Avvedimento EV, et al. Stimulatory autoantibodies to PDGF receptor in patients with extensive chronic graft-versus-host disease. *Blood.* 2007;110(1):237-41.
39. Celada LJ, Kropski JA, Herazo-Maya JD, Luo W, Creecy A, Abad AT, Chioma OS, Lee G, Hassell NE, Shaginurova GI, et al. PD-1 up-regulation on CD4(+) T cells promotes pulmonary fibrosis through STAT3-mediated IL-17A and TGF-beta1 production. *Sci Transl Med.* 2018; 10(460):eaar8356.
40. Shi J, Hou S, Fang Q, Liu X, Liu X, and Qi H. PD-1 Controls Follicular T Helper Cell Positioning and Function. *Immunity.* 2018;49(2):264-74 e4.
41. Wherry EJ, and Kurachi M. Molecular and cellular insights into T cell exhaustion. *Nat Rev Immunol.* 2015;15(8):486-99.
42. King C, Ilic A, Koelsch K, and Sarvetnick N. Homeostatic expansion of T cells during immune insufficiency generates autoimmunity. *Cell.* 2004;117(2):265-77.
43. Calzascia T, Pellegrini M, Lin A, Garza KM, Elford AR, Shahinian A, Ohashi PS, and Mak TW. CD4 T cells, lymphopenia, and IL-7 in a multistep pathway to autoimmunity. *Proc Natl Acad Sci U S A.* 2008;105(8):2999-3004.
44. Bennett L, Palucka AK, Arce E, Cantrell V, Borvak J, Banchereau J, and Pascual V. Interferon and granulopoiesis signatures in systemic lupus erythematosus blood. *J Exp Med.* 2003;197(6):711-23.
45. MacDonald KP, Rowe V, Filippich C, Johnson D, Morris ES, Clouston AD, Ferrara JL, and Hill GR. Chronic graft-versus-host disease after granulocyte colony-stimulating factor-mobilized allogeneic stem cell transplantation: the role of donor T-cell dose and differentiation. *Biol Blood Marrow Transplant.* 2004;10(6):373-85.
46. Levine JE, Wiley J, Kletzel M, Yanik G, Hutchinson RJ, Koehler M, and Neudorf S. Cytokine-mobilized allogeneic peripheral blood stem cell transplants in children result in rapid engraftment and a high incidence of chronic GVHD. *Bone Marrow Transplant.* 2000;25(1):13-8.
47. Johnston HF, Xu Y, Racine JJ, Cassady K, Ni X, Wu T, Chan A, Forman S, and Zeng D. Administration of anti-CD20 mAb is highly effective in preventing but ineffective in treating chronic graft-versus-host disease while preserving strong graft-versus-leukemia effects. *Biol Blood Marrow Transplant.* 2014;20(8):1089-103.
48. Serreze DV, Chapman HD, Niens M, Dunn R, Kehry MR, Driver JP, Haller M, Wasserfall C, and Atkinson MA. Loss of intra-islet CD20 expression may complicate efficacy of B-cell-directed type 1 diabetes therapies. *Diabetes.* 2011;60(11):2914-21.
49. Ryan CE, Sahaf B, Logan AC, O'Brien S, Byrd JC, Hillmen P, Brown JR, Dyer MJ, Mato AR, Keating MJ, et al. Ibrutinib efficacy and tolerability in patients with relapsed chronic lymphocytic leukemia following allogeneic HCT. *Blood.* 2016;128(25):2899-908.
50. Waller EK, Miklos D, Cutler C, Arora M, Jagasia MH, Pusic I, Flowers MED, Logan AC, Nakamura R, Chang S, et al. Ibrutinib for Chronic Graft-versus-Host Disease After Failure of Prior Therapy: 1-Year Update of a Phase 1b/2 Study. *Biol Blood Marrow Transplant*. 2019; 25(10):2002-2007.

Figures and figure legends:

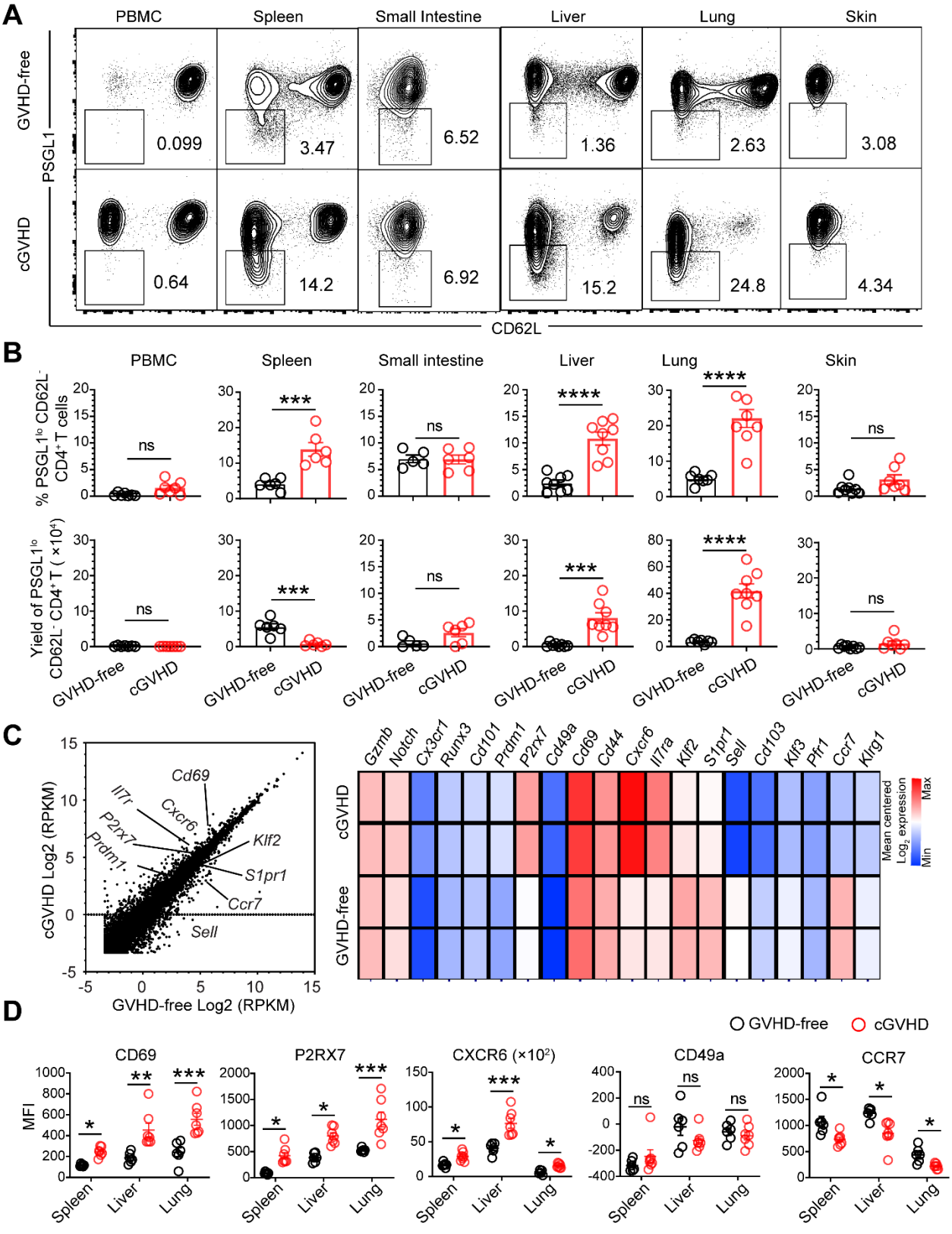

Figure 1: PSGL1^{lo}CD4^{+} T cells reside in the liver and lung. Lethally irradiated BACL/c (H-2^{d}) mice received TCD-BM plus splenocytes (cGVHD group) or TCD-BM alone (GVHD-free group) from C57BL/6 (H-2^{b}) donors. **(A)** 60 days after HCT, mononuclear cells (MNC) from the PBMC, spleen, small intestine, liver, lung, and skin were stained with anti-H-2Kb, TCRβ, CD4, CD62L and PSGL1. **(B)** Mean ± SEM of the percentage among donor-type CD4^{+} T cells and yield of donor-type H-2Kb^{+}PSGL1^{lo}CD62L^{-}CD4^{+}TCRβ^{+} cells are shown. N=6-8, combined from three replicate experiments. **(C)** Scatter plot comparing PSGL1^{lo}CD62L^{-}CD4^{+} T cells from GVHD-free and cGVHD recipients. The heatmap shown the core genes associated with tissue residency. Samples are pooled from 6-10 recipients of GVHD-free or cGVHD recipients, respectively. **(D)** Surface expression of CD69, P2RX7, CXCR6, CD49a and CCR7 of the PSGL1^{lo}CD62L^{-}CD4^{+} T cells was measured. Mean ± SEM of mean fluorescent intensity (MFI) is shown, N=6-8, combined from 3 independent experiments. P values were calculated by unpaired 2-tailed Student's t-tests **(B)** or by one-way ANOVA multiple-comparisons **(D).** * p<0.05; ** p<0.01; *** p<0.001; **** p<0.0001.

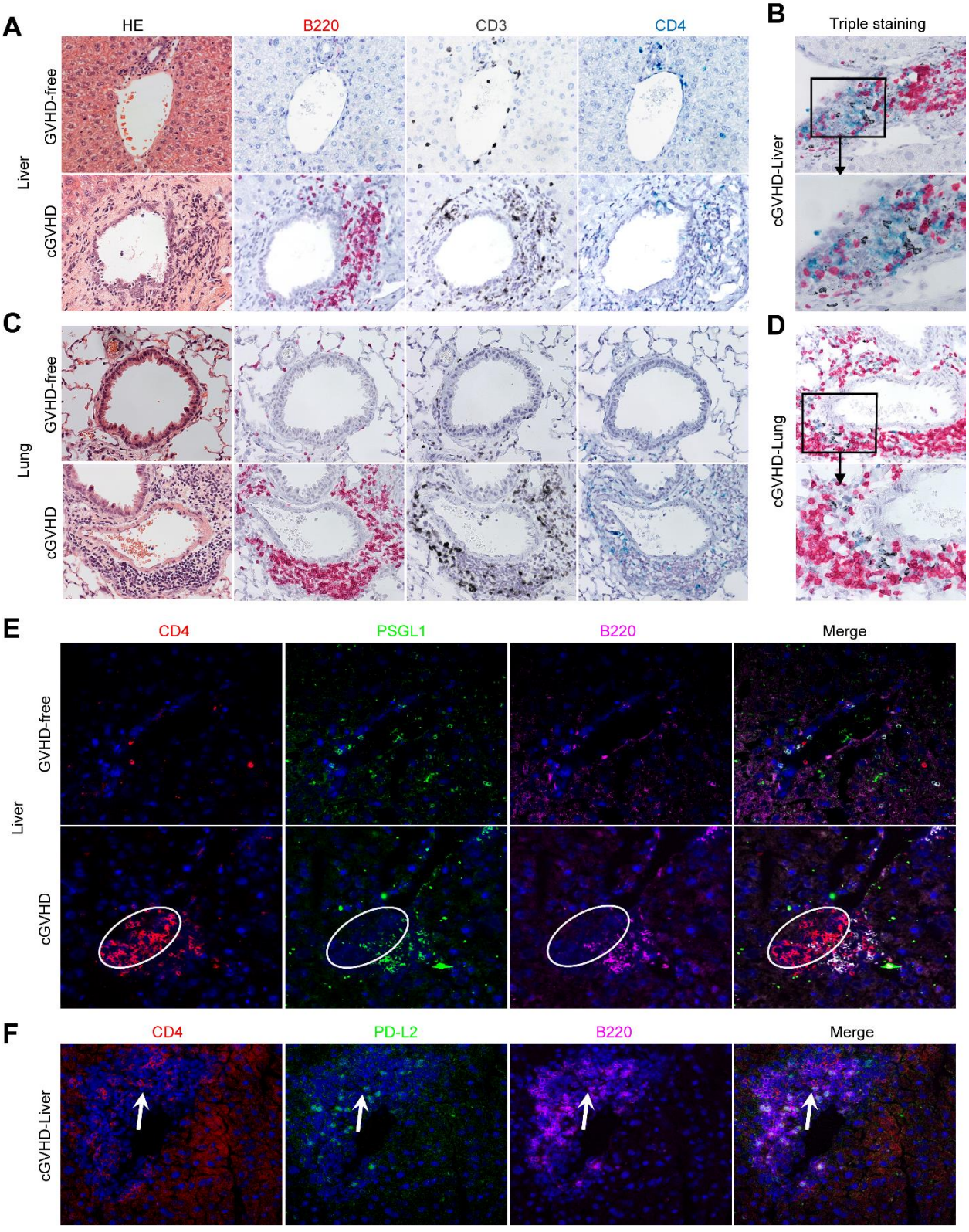
A
HE
B220
CD3
CD4
Liver
GVHD-free
cGVHD
B
Triple staining
cGVHD-Liver
C
Lung
GVHD-free
cGVHD
D
cGVHD-Lung
E
CD4
PSGL1
B220
Merge
Liver
GVHD-free
cGVHD
F
CD4
PD-L2
B220
Merge
cGVHD-Liver

Figure 2: Adjoining PSGL1^{lo}CD4^{+} T cells and B cells are present in cGVHD target tissues. 60 days after HCT, liver **(A and B)** and lung **(C and D)** tissues of recipients given C57BL/6 TCD-BM alone or with splenic Thy1.2 T cells were stained with immunochemistry for B220, CD3 and CD4 separately or together (original magnification, ×400; **B and D** bottom panel magnification, ×630). **(E)** Liver sections were also stained with immunofluorescent mAb for CD4, PSGL1 and B220. The oval demarcates a region of accumulated PSGL1^{lo}CD4^{+}T cells that co-localize with B220^{+} B cells. **(F)** Liver sections were stained with antibodies against CD4, PD-L2 and B220. Arrows show PD-L2^{+} B cells adjacent to CD4^{+} cells (**E and F**, original magnification, ×200). One representative experiment of 4 replicates is shown.

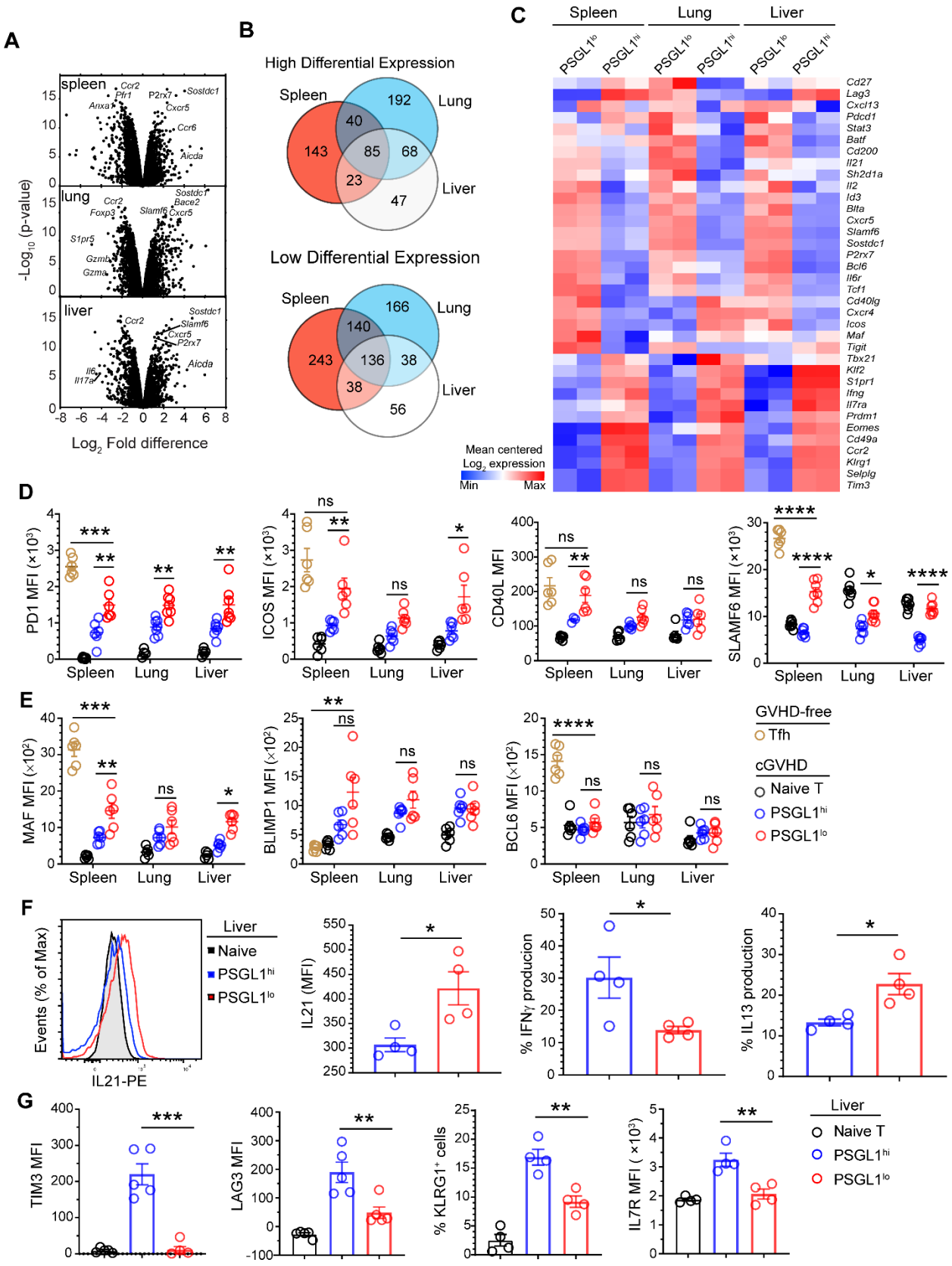
A
spleen
lung
liver
-Log10 (p-value)
Log2 Fold difference
B
High Differential Expression
Spleen
Lung
Liver
192
40
143
85
68
23
47
Low Differential Expression
166
140
243
136
38
38
56
C
Spleen
Lung
Liver
PSGL1lo
PSGL1hi
Cd27
Lag3
Cxcl13
Pdcd1
Stat3
Batf
Cd200
Il21
Sh2d1a
Il2
Id3
Blta
Cxcr5
Slamf6
Sostdc1
P2rx7
Bcl6
Il6r
Tcf1
Cd40lg
Cxcr4
Icos
Maf
Tigit
Tbx21
Klf2
S1pr1
Ifng
Il7ra
Prdm1
Eomes
Cd49a
Ccr2
Klrg1
Selplg
Tim3
Mean centered Log2 expression
Min
Max
D
PD1 MFI (×10³)
ICOS MFI (×10³)
CD40L MFI
SLAMF6 MFI (×10³)
E
MAF MFI (×10²)
BLIMP1 MFI (×10²)
BCL6 MFI (×10²)
GVHD-free
Tfh
cGVHD
Naive T
PSGL1hi
PSGL1lo
F
Events (% of Max)
IL21-PE
Liver
Naive
PSGL1hi
PSGL1lo
IL21 (MFI)
% IFNγ producion
% IL13 production
G
TIM3 MFI
LAG3 MFI
% KLRG1+ cells
IL7R MFI (×10³)
Liver
Naive T
PSGL1hi
PSGL1lo

Figure 3: Tissue-resident PSGL^{lo}CD4^{+} T cells are B cell helpers. PSGL1^{lo} and PSGL1^{hi} CD62L^{-} CD4^{+} T cells from the spleen, lung, and liver of cGVHD recipients were sorted for RNA sequencing at 30 days after HCT. **(A)** Volcano plot of all gene expression levels between PSGL1^{hi} and PSGL1^{lo} CD4^{+} T cells. **(B)** Numbers of genes with high and low differential expression in PSGL1^{lo} CD4^{+} T cells as compared with PSGL1^{hi} CD4^{+} T cells. **(C)** The heatmap analysis of clustered genes related to B cell-helper features by PSGL1^{hi} and PSGL1^{lo} CD4^{+} T cells. **(D)** Surface expression levels of PD1, ICOS, CD40L and SLAMF6 among naïve CD4^{+} T cells, Tfh cells, PSGL1^{lo} and PSGL1^{hi} CD4^{+} T cells. **(E)** Intracellular expression levels of MAF, BLIMP1 and BCL6. **(F)** Sorted PSGL1^{lo}CD4^{+} T cells from the liver tissue were stained for intracellular IL21, IFNγ and IL13. Mean ± SEM of MFI is shown for IL21, and percentages for IFNγ^{+} and IL13^{+} cells. **(G)** Surface expression of T cell anergy/exhaustion-related receptors TIM3, LAG3, KLRG1, and IL7R. Mean ± SEM of MFI is shown, N=4-7 combined from at least two replicate experiments. P values were calculated by unpaired 2-tailed Student's t-tests **(D, E, and F)** or one-way ANOVA multiple-comparisons **(G).** *p<0.05; **p<0.01; ***p<0.001; ****p<0.0001.

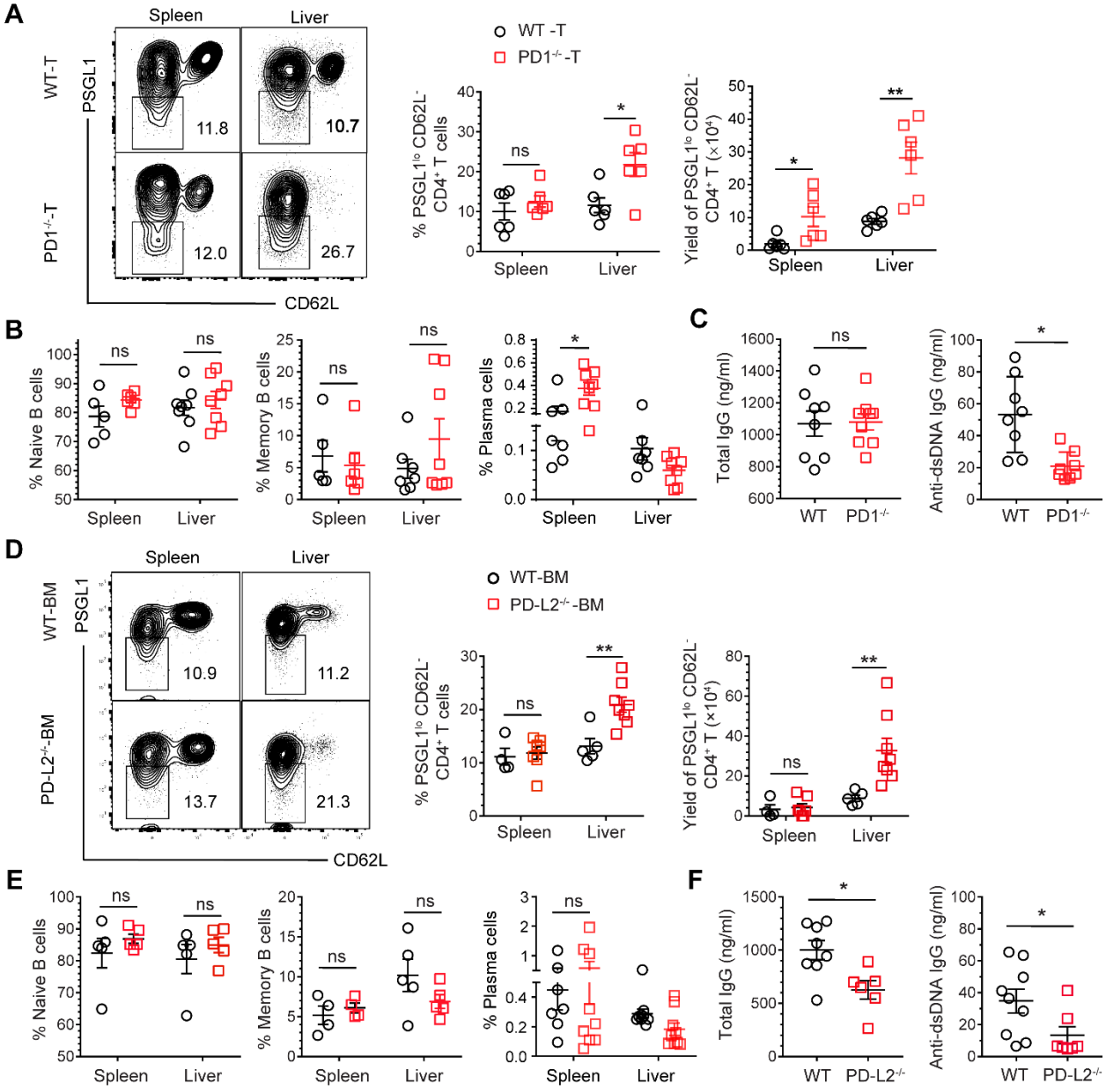
A
Spleen
Liver
WT-T
PD1-/--T
PSGL1
CD62L
11.8
10.7
12.0
26.7
WT -T
PD1-/- -T
% PSGL1lo CD62L- CD4+ T cells
Yield of PSGL1lo CD62L- CD4+ T (×10⁴)
ns
*
**
B
% Naive B cells
% Memory B cells
% Plasma cells
C
Total IgG (ng/ml)
Anti-dsDNA IgG (ng/ml)
WT
PD1-/-
D
WT-BM
PD-L2-/--BM
10.9
11.2
13.7
21.3
E
F
PD-L2-/-

Figure 4: PD1 deficiency in T cells and PD-L2 deficiency in B cells enhances expansion of PSGL1^{lo}CD4^{+} T cells in the liver but reduces autoantibody production. Lethally irradiated BALB/c mice received Thy1.2^{+} T cells from PD1$^{-/-}$ donors and TCD-BM from wild-type (WT) donors **(A-C)** or Thy1.2^{+} T cells from WT donors and TCD-BM from PD-L2$^{-/-}$ donors **(D-F).** At day 60 after HCT, recipients were evaluated for percentage of donor-type PSGL1^{lo}CD4^{+} T cells among donor-CD4^{+} T cells, absolute numbers of donor-type PSGL1^{lo}CD4^{+} T cells, and percentages of CD19^{+}IgD^{+}CD80^{-} naïve B cells, CD19^{+}IgD^{-}CD80^{+}PD-L2^{+} and CD19^{+}IgD^{-}CD80^{+}CD73^{+} memory B cells, and CD19$^{lo/-}$CD138^{+} plasma cells among CD19^{+} B cells in the spleen and liver. Mean ± SEM is shown, N=5-8, combined from 2 independent experiments. **(A)** Percentage and yield of PSGL1^{lo}CD4^{+} T cells in the recipients given WT or PD1$^{-/-}$ T cells. **(B)** Percentage of naïve B, memory B and plasma cells. **(C)** Serum total IgG and anti-ds DNA IgG autoantibody concentration detected by ELISA. **(D)** Percentages and yield of PSGL1^{lo}CD4^{+} T cells in the recipients given WT T or PD-L2$^{-/-}$ TCD-BM cells. **(E)** Percentage of naïve B, memory B, and plasma cells. **(F)** Serum concentrations of total IgG and anti-dsDNA IgG autoantibodies. P values were calculated by one-way ANOVA multiple-comparisons **(A, B, D, E)** and unpaired 2-tailed Student's t-tests **(C, F)**. *p<0.05; **p<0.01; ***p<0.001.

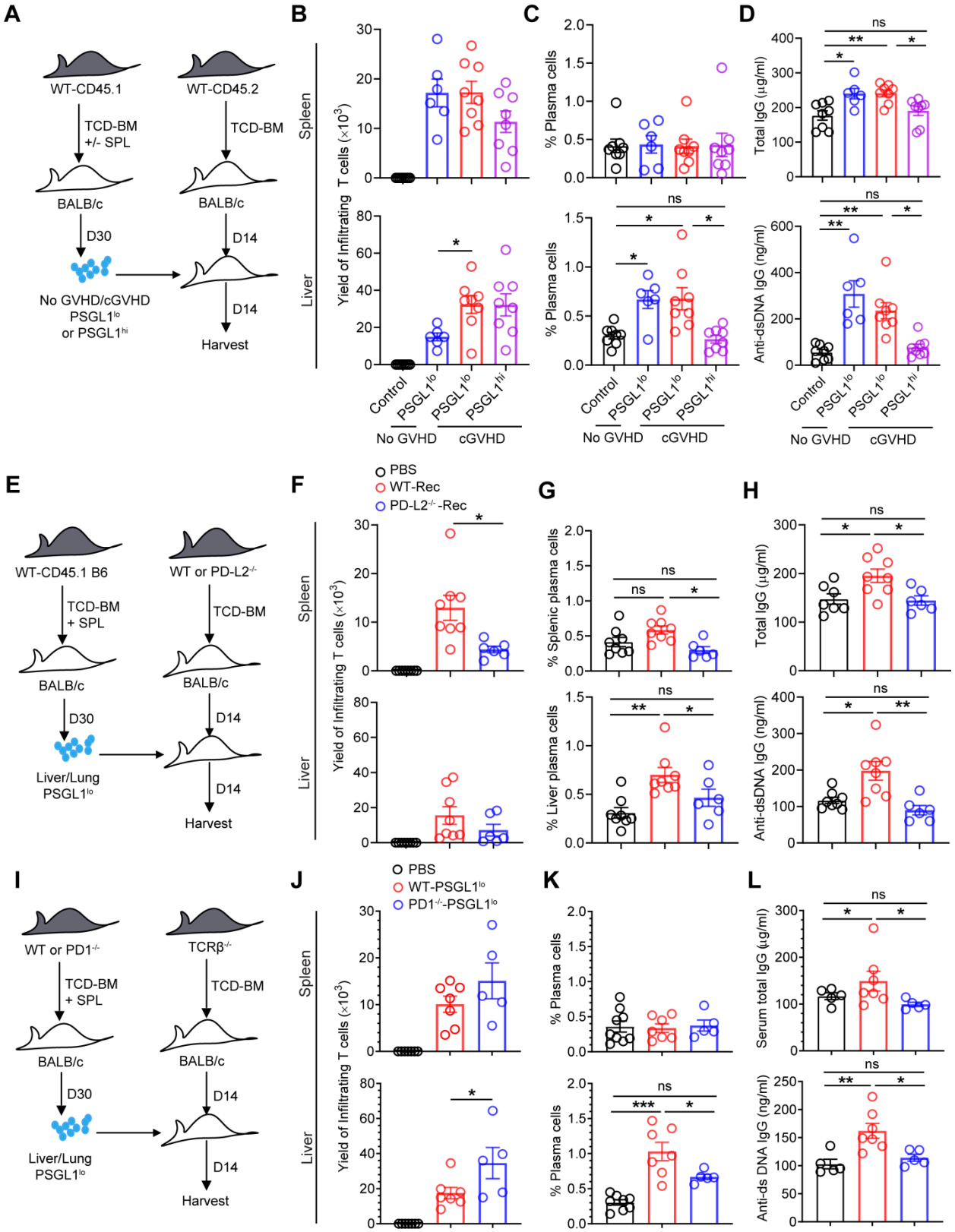
A
WT-CD45.1
WT-CD45.2
TCD-BM +/- SPL
TCD-BM
BALB/c
BALB/c
D30
D14
No GVHD/cGVHD PSGL1lo or PSGL1hi
D14
Harvest
B
Spleen
Liver
Yield of Infiltrating T cells (×10³)
Control
PSGL1lo
PSGL1lo
PSGL1hi
No GVHD
cGVHD
C
% Plasma cells
ns
D
Total IgG (μg/ml)
Anti-dsDNA IgG (ng/ml)
E
WT-CD45.1 B6
WT or PD-L2-/-
TCD-BM + SPL
TCD-BM
BALB/c
BALB/c
D30
D14
Liver/Lung PSGL1lo
D14
Harvest
F
PBS
WT-Rec
PD-L2-/--Rec
G
% Splenic plasma cells
% Liver plasma cells
H
Total IgG (μg/ml)
Anti-dsDNA IgG (ng/ml)
I
WT or PD1-/-
TCRβ-/-
TCD-BM + SPL
TCD-BM
BALB/c
BALB/c
D30
D14
Liver/Lung PSGL1lo
D14
Harvest
J
PBS
WT-PSGL1lo
PD1-/--PSGL1lo
K
% Plasma cells
L
Serum total IgG (μg/ml)
Anti-ds DNA IgG (ng/ml)

Figure 5: PSGL1^{lo}CD4^{+} T cell PD1 interaction with B cell PD-L2 augments B cell differentiation to plasma cells and IgG autoantibody production in adoptive transfer recipients. cGVHD was induced in BALB/c recipients by transplanting CD45.1^{+} TCD-BM alone or together with splenocytes from C57BL/6 donors. 30 days after HCT, donor-type PSGL1^{lo}CD62L^{-} CD4^{+} T cells and PSGL1^{hi}CD62L^{-} CD4^{+} T cells were sorted and adoptively transferred into irradiated BALB/c chimeras grafted with TCD-BM from C57BL/6 WT donors 14 days previously. 14 days after the adoptive transfer, numbers of the injected PSGL1^{lo}CD62L^{-} CD4^{+} T cells and percentages of CD19$^{lo/-}$CD138^{+} plasma cells among total donor CD19^{+} B cells in the spleen and liver were analyzed, and serum concentrations of total IgG and anti-dsDNA IgG were measured. Mean ± SEM is shown, N= 5-8 combined from at least two replicate experiments. **(A-D)** Transfer of GVHD-free spleen-derived PSGL1^{lo}CD62L^{-} cells, GVHD liver and lung-derived PSGL1^{lo}CD62L^{-} or PSGL1^{hi}CD62L^{-} CD4^{+} T cells into adoptive recipients with WT B cells. **(E-H)** Transfer of WT PSGL1^{lo}CD62L^{-} CD4^{+} T cells into adoptive recipients with PD-L2$^{-/-}$ B cells. **(I-L)** Transfer of WT or PD1$^{-/-}$ PSGL1^{lo}CD62L^{-} CD4^{+} T cells into adoptive recipients with WT B cells. P values were calculated by one-way ANOVA multiple-comparisons **(C, G, K)** or multiple t-tests **(B, D, F, H, J, L)**. *p<0.05; **p<0.01; ***p<0.001.

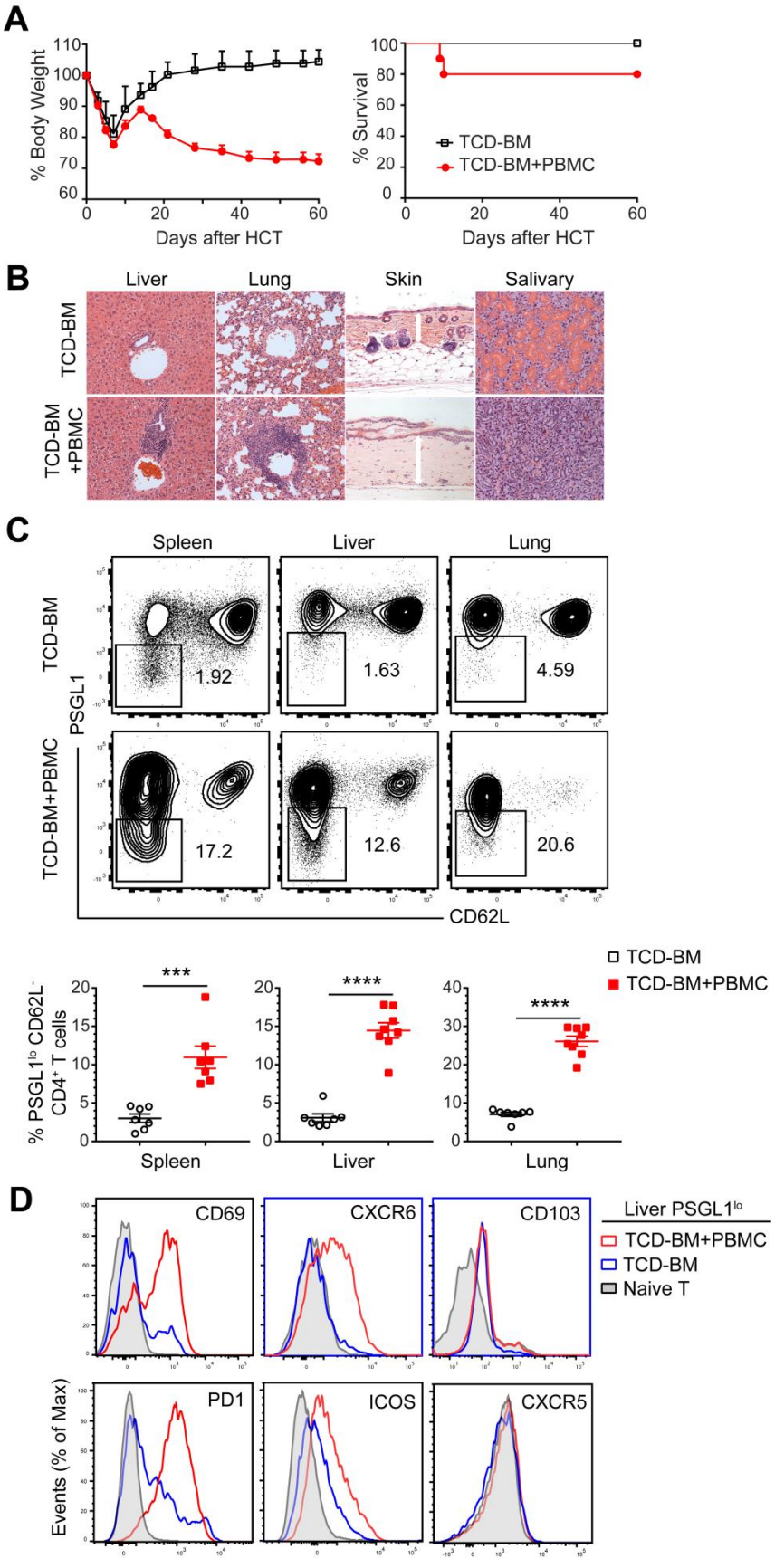
A
% Body Weight
Days after HCT
% Survival
TCD-BM
TCD-BM+PBMC
B
Liver
Lung
Skin
Salivary
TCD-BM
TCD-BM +PBMC
C
Spleen
Liver
Lung
TCD-BM
TCD-BM+PBMC
PSGL1
CD62L
1.92
1.63
4.59
17.2
12.6
20.6
% PSGL1lo CD62L- CD4+ T cells
***
****
****
D
CD69
CXCR6
CD103
Liver PSGL1lo
TCD-BM+PBMC
TCD-BM
Naive T
PD1
ICOS
CXCR5
Events (% of Max)

Figure 6: Donor PBMC PSGL1^{hi}CD4^{+} T cells give rise to PSGL1^{lo}CD4^{+} T cells in cGVHD recipients. cGVHD was induced in BALB/c recipients by transplanting PBMC and TCD-BM cells from C57BL/6 donors. 60 days after HCT, donor-type T cells were analyzed for percentage of PSGL1^{lo}CD62L^{-}CD4^{+} T cells, which were further analyzed for expression of tissue-resident markers (CD69, CXCR6 and CD103) and B cell helper markers (PD1, ICOS and CXCR5). **(A)** Curves of %Survivor and %body weight change. N=10, combined from two replicate experiments. **(B)** H&E staining of liver, lung, skin and salivary gland. One representative micrograph is shown of 6 in each group (original magnification, ×200). **(C)** Representative flow cytometry patterns of PSGL1 versus CD62L after gating on H-2b^{+}TCRβ^{+}CD4^{+} T cells and Mean ± SEM of %PSGL1^{lo}CD62L^{-}CD4^{+} T cells in the spleen, liver and lung. N=7. **(D)** Surface expression of CD69, CXCR6, CD103, PD1, ICOS and CXCR5 among naïve CD4^{+} T cells from donors and PSGL1^{lo}CD62L^{-}CD4^{+} T cells from GVHD-free recipients and from cGVHD recipients. One representative histogram is shown of 6 in each group. P values were calculated by unpaired 2-tailed Student's t-tests. *p<0.05; **p<0.01; ***p<0.001.

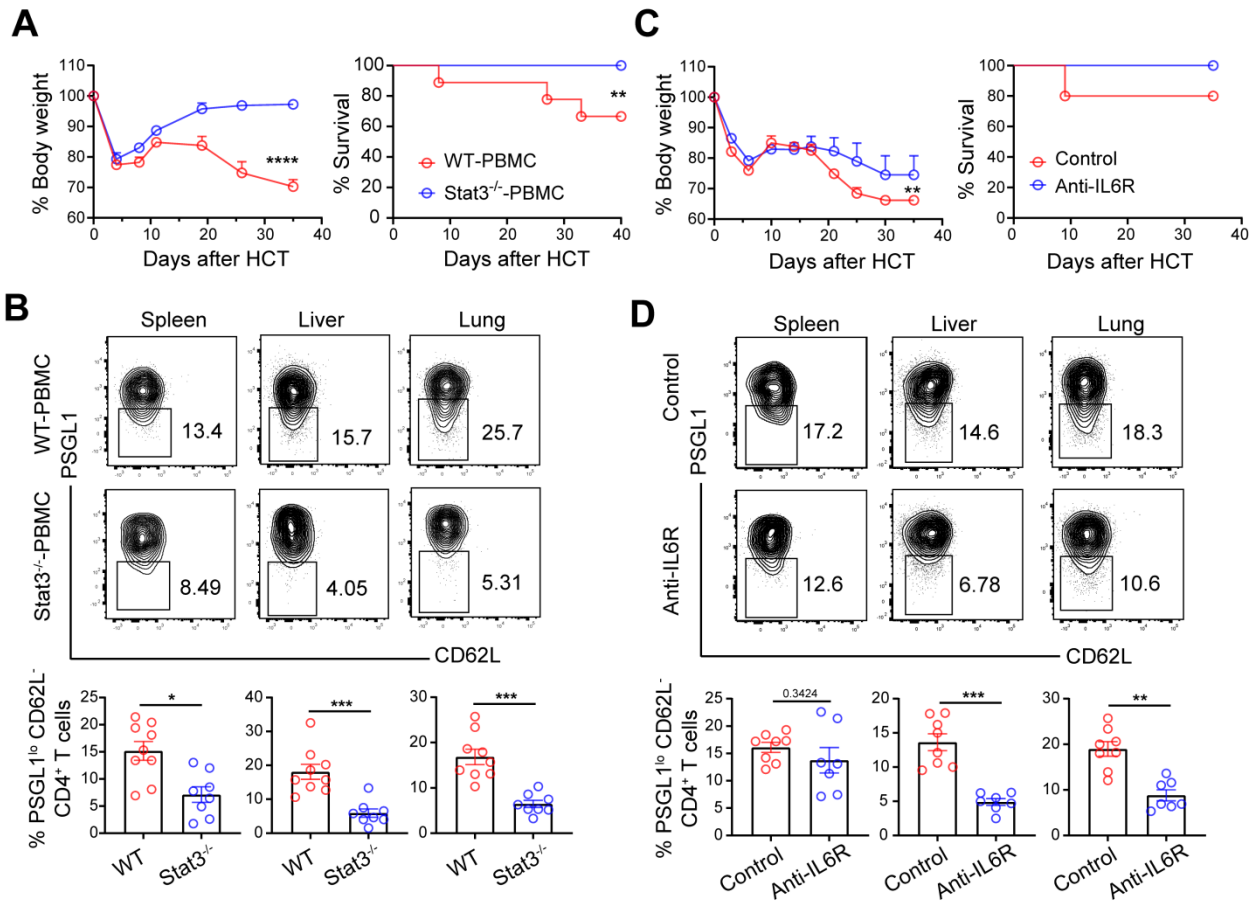
A
% Body weight
Days after HCT
****
% Survival
WT-PBMC
Stat3-/--PBMC
**
C
% Body weight
**
% Survival
Control
Anti-IL6R
B
Spleen
Liver
Lung
WT-PBMC
PSGL1
13.4
15.7
25.7
Stat3-/--PBMC
8.49
4.05
5.31
CD62L
% PSGL1lo CD62L- CD4+ T cells
WT
Stat3-/-
D
Control
Anti-IL6R
17.2
14.6
18.3
12.6
6.78
10.6
0.3424

Figure 7: PSGL1^{hi}CD4^{+} T cells differentiate into PSGL1^{lo}CD4^{+} T cells in an IL6R-Stat3-dependent- manner. BALB/c recipients were given 0.5M PBMCs from WT or Stat3-/- donors plus 2.5M TCD-BM from CD45.1 donors, and tissues were harvested at day 40 after HCT. **(A)** Curves of %body weight changes and %survivor. **(B)** Mononuclear cells (MNC) from the spleen, liver and lung were stained with anti-H-2Kb, CD45.1, TCRβ, CD4, CD62L and PSGL1. Mean ± SEM of the percent donor-type H-2Kb^{+}PSGL1^{lo}CD62L^{-}CD4^{+}CD45.1^{-}TCRβ^{+} among donor-type CD4^{+} T cells is shown. N=8-10, combined from at least 2 replicate experiments. **(C)** Recipients were treated with anti-IL6R mAbs or control IgG weekly, and tissues were harvested 40 days after HCT. Curves of %body weight changes and %survivor. **(D)** Percentages of donor type of H-2Kb^{+}PSGL1^{lo}CD62L^{-}CD4^{+}CD45.1^{-}TCRβ^{+} cells among donor-type CD4^{+} T cells are shown. N=6-8, combined from 2 replicate experiments. P values were calculated by correlation test or log-rank test **(A, C)** or unpaired 2-tailed Student's t-tests **(B, D)**. *p<0.05; **p<0.01; ***p<0.001.

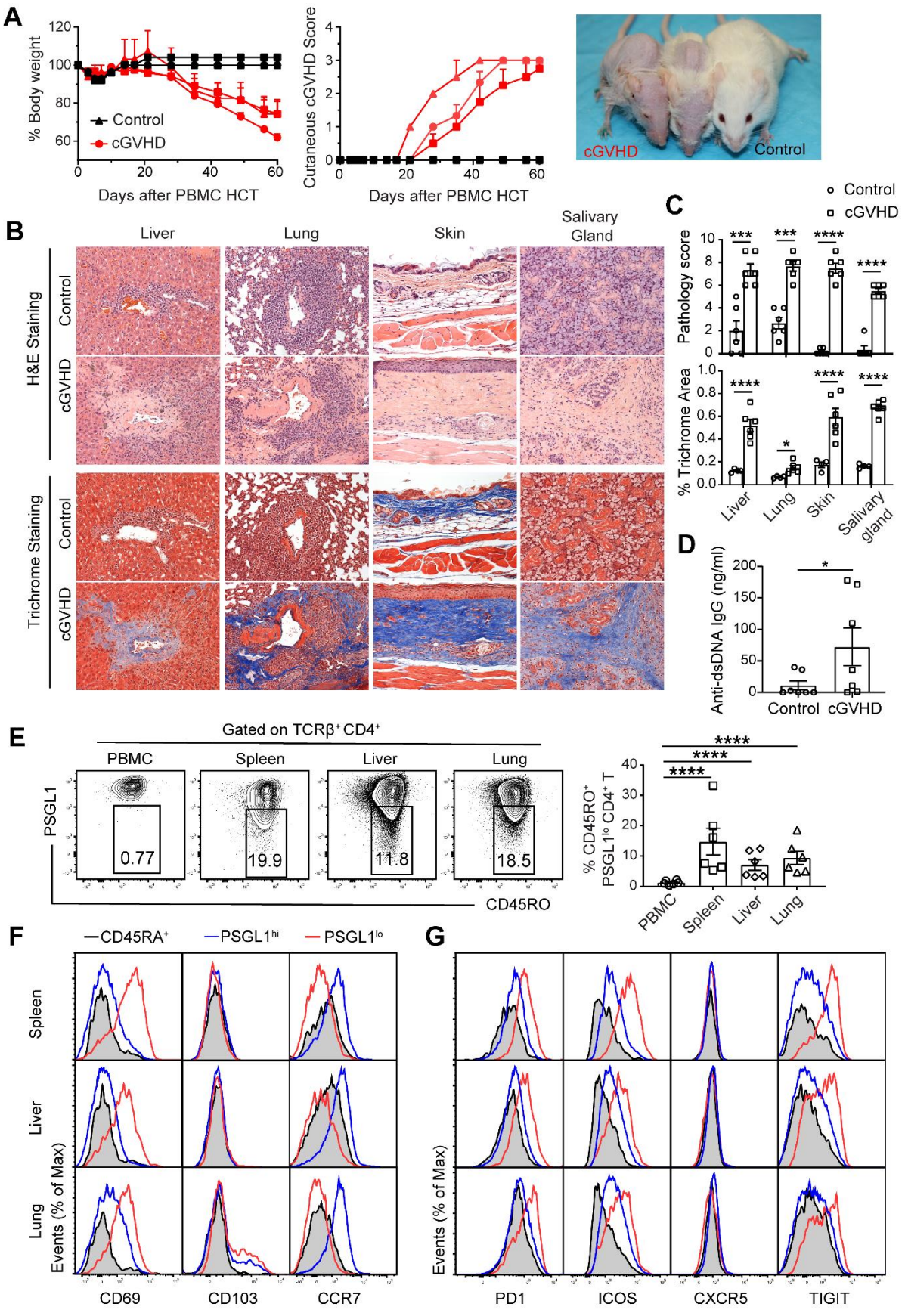
A
% Body weight
Control
cGVHD
Days after PBMC HCT
Cutaneous cGVHD Score
Days after PBMC HCT
cGVHD
Control
B
Liver
Lung
Skin
Salivary Gland
H&E Staining
Trichrome Staining
Control
cGVHD
C
Control
cGVHD
Pathology score
% Trichrome Area
Liver
Lung
Skin
Salivary gland
D
Anti-dsDNA IgG (ng/ml)
Control
cGVHD
E
Gated on TCRβ+ CD4+
PBMC
Spleen
Liver
Lung
PSGL1
CD45RO
0.77
19.9
11.8
18.5
% CD45RO+ PSGL1lo CD4+ T
F
CD45RA+
PSGL1hi
PSGL1lo
Spleen
Liver
Lung
Events (% of Max)
CD69
CD103
CCR7
G
PD1
ICOS
CXCR5
TIGIT

Figure 8: Human PBMC gives rise to tissue-resident PSGL1^{lo}CD4^{+} T cells in humanized cGVHD mice. MHC$^{-/-}$ NSG or MHC$^{-/-}$HLA-A2^{+}DR4^{+} NSG mice were treated with 200 cGy TBI followed by injection of freshly isolated PBMC from 3 HLA-A2^{-}DR4^{-} donors. PBMC from 3 donors were injected into 3 mice each. Recipients were monitored for development of GVHD for up to 60 days after HCT **(A)** Curves of %body weight changes and cutaneous GVHD score and representative photographs of 1 GVHD-free MHC$^{-/-}$ mouse and 2 GVHD MHC$^{-/-}$HLA-A2^{+}DR4^{+} mice given the same human PBMC. **(B)** Representative H&E and trichrome stains of liver, lung, skin and salivary gland (original magnification, ×200). **(C)** Mean ± SEM of pathology score and trichrome staining areas. **(D)** Serum anti-dsDNA IgG concentration. **(E)** Representative flow cytometry patterns and Mean ± SEM of %PSGL1^{lo}CD4^{+} T cells. **(F & G)** Surface marker expression of CD69, CCR7, CD103, PD1, ICOS, CXCR5 and TIGIT by PSGL1^{lo} in comparison to PSGL1^{hi} T cells from spleen, liver and lung of GVHD HLA-A2^{+}DR4^{+} NSG recipients. One representative of 3 replicate experiments is shown. P values were calculated by one-way ANOVA **(C, E)** or unpaired 2-tailed Student's t-tests **(D)**. *p<0.05; **p<0.01; ***p<0.001.

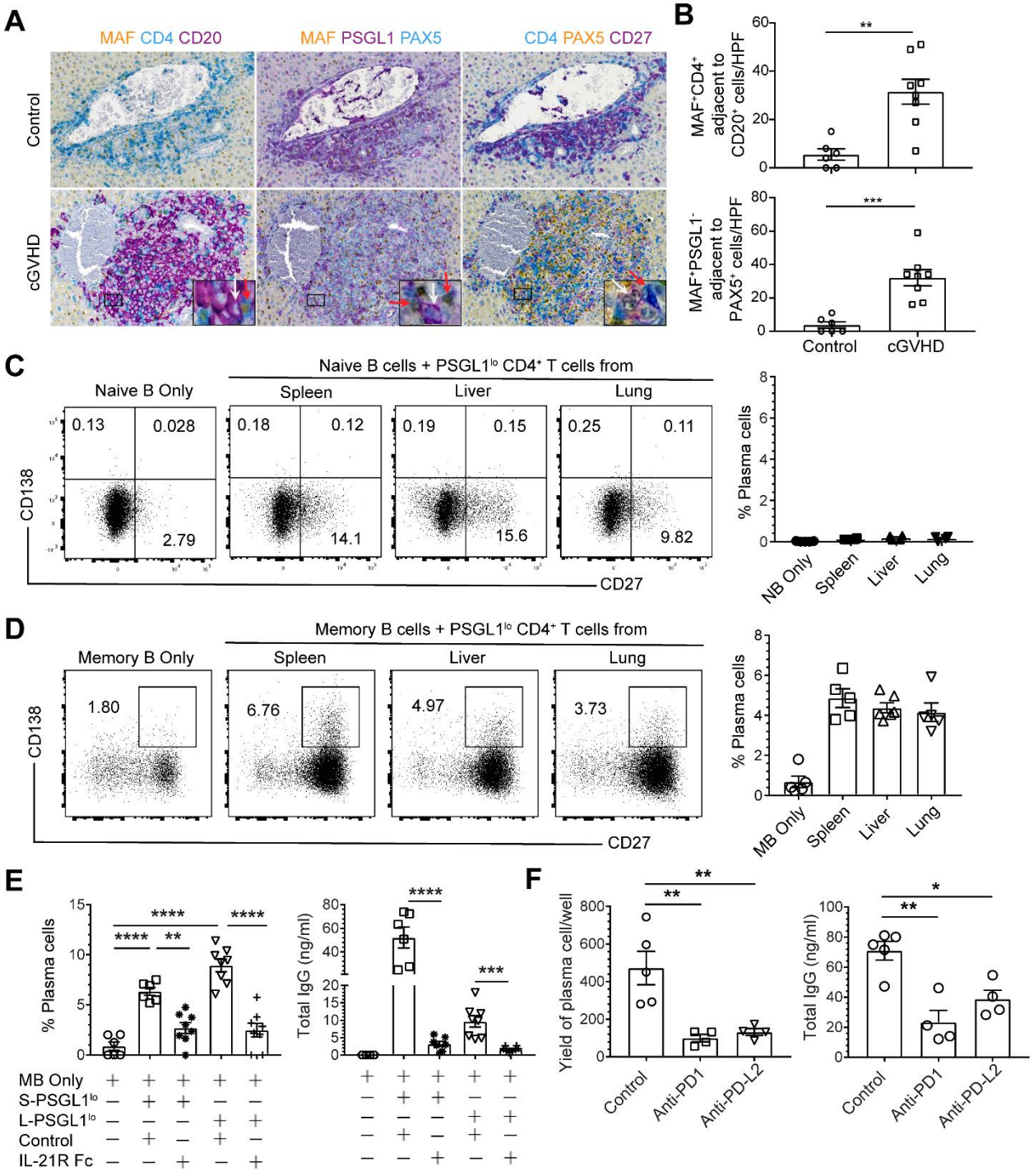
A
MAF CD4 CD20
MAF PSGL1 PAX5
CD4 PAX5 CD27
Control
cGVHD
B
MAF+CD4+ adjacent to CD20+ cells/HPF
MAF+PSGL1- adjacent to PAX5+ cells/HPF
Control
cGVHD
C
Naive B Only
Naive B cells + PSGL1lo CD4+ T cells from
Spleen
Liver
Lung
0.13
0.028
2.79
0.18
0.12
14.1
0.19
0.15
15.6
0.25
0.11
9.82
CD138
CD27
% Plasma cells
NB Only
Spleen
Liver
Lung
D
Memory B Only
Memory B cells + PSGL1lo CD4+ T cells from
Spleen
Liver
Lung
1.80
6.76
4.97
3.73
CD138
CD27
% Plasma cells
MB Only
Spleen
Liver
Lung
E
% Plasma cells
Total IgG (ng/ml)
MB Only
S-PSGL1lo
L-PSGL1lo
Control
IL-21R Fc
F
Yield of plasma cell/well
Total IgG (ng/ml)
Control
Anti-PD1
Anti-PD-L2

Figure 9: Human PBMC-derived tissue-resident PSGL1^{lo}CD4^{+} T cells augment autologous memory B cell differentiation into plasma cells with IgG antibody production. Humanized cGVHD mice were established as in Figure 8. **(A)** Adjacent three sections of liver tissues of control and cGVHD mice were stained with 1) anti-human MAF, CD4 and CD20; 2) anti-human MAF, PSGL1 and PAX5; or 3) anti-human CD4, PAX5 and CD27. White arrows point to B cells and red arrows point to T cells in different panels (original magnification, ×200; insets, ×800). **(B)** Quantification of total MAF^{+}CD4^{+} T and MAF^{+}PSGL1^{-} T adjacent to B cells in the liver tissues. (**C-F**) Human PSGL1^{lo}CD45RO^{+}CD4^{+} T cells from the spleen, liver and lung of humanized cGVHD HLA-A2^{+}DR4^{+} NSG recipients 60 days after cell transfer were sorted and co-cultured with sorted autologous naïve or memory B cells from cryopreserved PBMC. **(C)** Naïve B cells alone or co-cultured with PSGL1^{lo}CD4^{+} T cells from spleen, liver or lung. Representative flow cytometry staining patterns of CD27 versus CD138 on B cells and percentages of plasma cells are shown. **(D)** Memory B cells alone or co-cultured with PSGL1^{lo}CD4^{+} T cells from spleen, liver or lung. Representative flow cytometry patterns and percentages of plasma cells are shown. **(E)** Memory B cells co-cultured with PSGL1^{lo}CD4^{+} T cells with or without neutralization of IL-21 with IL-21R-Fc. Percentage of plasma cells and IgG concentrations in culture supernatants are shown. **(F)** Memory B cells co-cultured with PSGL1^{lo}CD4^{+} T cells with or without blocking anti-PD1 or anti-PD-L2. Yields of plasma cells and total IgG levels are shown. Each experiment was repeated at least twice. P values were calculated by unpaired 2-tailed Student's t-tests **(B)** or one-way ANOVA multiple-comparisons **(E, F)**. *p<0.05; **p<0.01; ***p<0.001; **** p<0.0001.

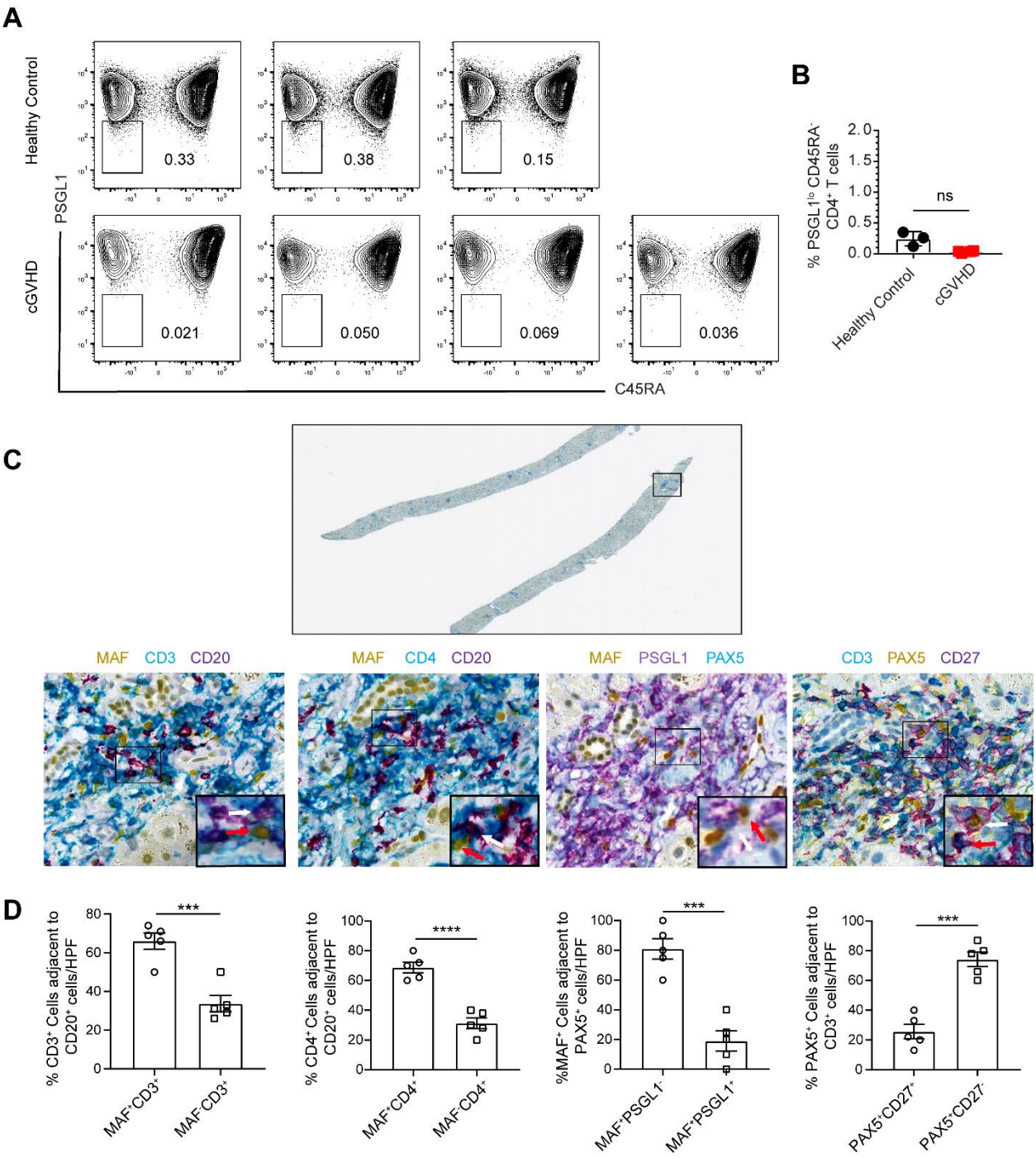
A
Healthy Control
cGVHD
PSGL1
C45RA
0.33
0.38
0.15
0.021
0.050
0.069
0.036
B
% PSGL1lo CD45RA- CD4+ T cells
ns
Healthy Control
cGVHD
C
MAF CD3 CD20
MAF CD4 CD20
MAF PSGL1 PAX5
CD3 PAX5 CD27
D
% CD3+ Cells adjacent to CD20+ cells/HPF
MAF+CD3+
MAF-CD3+
% CD4+ Cells adjacent to CD20+ cells/HPF
MAF+CD4+
MAF-CD4+
%MAF+ Cells adjacent to PAX5+ cells/HPF
MAF+PSGL1-
MAF+PSGL1+
% PAX5+ Cells adjacent to CD3+ cells/HPF
PAX5+CD27-
PAX5+CD27+

Figure 10: PSGL1^{lo} MAF^{+} CD4^{+} T cells and CD27^{+} memory B cells accumulate in the liver lesions of cGVHD patients. (A) PBMC from healthy control and cGVHD patient were stained with anti-human CD3, anti-human CD4, anti-human CD45RA and anti-human PSGL1. Flow cytometry staining patterns of 3 healthy controls and 4 cGVHD patients, and **(B)** the mean ± SEM of percentage of PSGL1^{lo}CD45RA^{-}CD4^{+} T cells are shown. **(C)** Immunohistochemistry staining of 4 adjacent slides of liver biopsy tissues from cGVHD patient with 1) anti-human MAF, CD3 and CD20; 2) anti-human MAF, CD4 and CD20; 3) anti-human Maf, PSGL1 and PAX5; or 4) anti-human CD3, PAX5 and CD27. Representative result of one patient is shown for 5 cGVHD patients. White arrows point to B cells, and red arrows point to T cells (original magnification, ×400; insets, ×800). **(D)** Calculation of percentage of MAF^{+} T subsets or PAX5^{+} B cell subset that were juxtaposed to each other. P value was calculated by unpaired 2-tailed Student's t-tests **(B, D)**. *p<0.05; **p<0.01; ***p<0.001; **** p<0.0001.

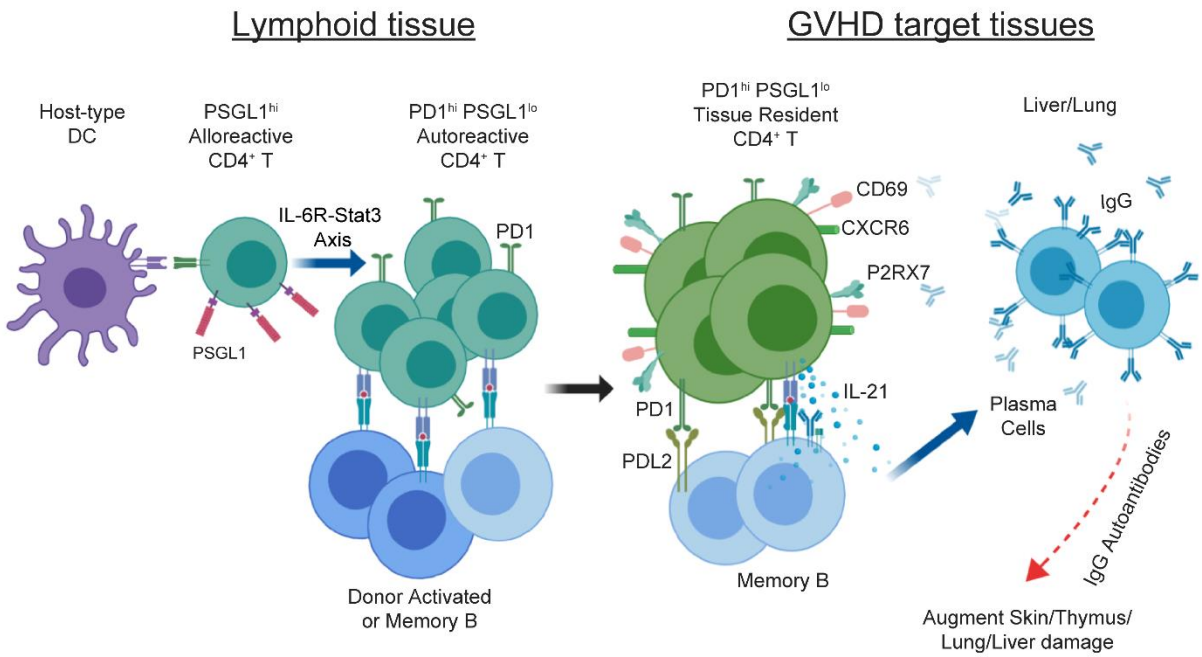

Figure 11: Summary Diagram describing the development of tissue resident PSGL1^{lo}CD4^{+} T cells and their interaction with B cells in GVHD target tissues.